Supplementary Online Material (SOM):

A late Neanderthal tooth from northeastern Italy

SOM S1

DNA extraction, library preparation and enrichment for mitochondrial DNA

The tooth from Riparo Broion was sampled in the clean room of the University of Bologna in Ravenna, Italy. After removing a thin layer of surface material, the tooth was drilled adjacent to the cementoenamel junction using 1.0 mm disposable dental drills. Approximately 50 mg of tooth powder were collected.

All subsequent laboratory steps were performed at the Max Planck Institute for Evolutionary Anthropology in Leipzig, Germany, using automated liquid handling systems (Bravo NGS workstation, Agilent Technologies) as described in Rohland et al. (2018) for DNA extraction and in Slon et al. (2017b) for other procedures. Negative controls for the extraction and library preparation steps accompanied the sample throughout the process (SOM Table S7).

To generate a lysate, 500 µl of lysis buffer (0.45M EDTA, pH 8.0, 0.25mg/mL Proteinase K, 0.05% Tween-20) was added to ~5 mg of tooth powder (Dabney et al., 2013; Korlevic et al., 2015). Initially, one 150 µl aliquot was purified by binding the DNA to silica magnetic beads with binding buffer 'D' (Dabney et al., 2013; Rohland et al., 2018). In order to generate additional data, two additional aliquots of the lysate were later purified using the same procedure.

Each extract was converted into a single-stranded DNA library (Gansauge et al., 2017), and qPCR assays were carried out to quantify the number of molecules in the libraries (Gansauge and Meyer, 2013) and to evaluate the efficiency of the library preparation procedure (Glocke and Meyer, 2017; SOM Table S7). Each library was then tagged with a pair of unique 7 bp-indices (Kircher et al., 2012) with the modifications in (Korlevic et al., 2015)). After amplification to plateau with AccuPrime Pfx DNA polymerase (Life Technologies; Dabney and Meyer, 2012), the DNA libraries were purified using SPRI beads (DeAngelis et al., 1995) as described in Slon et al. (2017b). Note that for the second library preparation setup, the concentration of PEG-8000 in the SPRI beads mix was reduced from 38% to 28% (w/v).

Approximately 1 µg of DNA from each library was enriched for human mitochondrial DNA fragments using probes spanning the complete mitochondrial genome sequence of the revised Cambridge Reference Sequence (rCRS, Andrews et al., 1999), generated as described in Fu et al.

(2013a). Two rounds of an on-bead hybridization capture procedure were performed (Maricic et al., 2010), as modified in Slon et al. (2017b). The enriched libraries, along with their relevant negative controls, were pooled with libraries stemming from other projects and underwent paired-end sequencing in 76 cycles (Kircher et al., 2012) on a MiSeq platform (Illumina).

SOM S2

Data generation and data processing

We used Bustard to perform base calling (Bentley et al., 2008) and leeHom to remove adapters and merge overlapping forward and reverse reads (Renaud et al., 2014). We assigned sequences to individual sample libraries requiring a perfect match of the index sequences to the expected barcode combinations. We then aligned sequences to the rCRS (Andrews et al., 1999) with a Burrows-Wheeler Aligner (BWA; Li and Durbin, 2010) using parameters for ancient DNA "-n 0.01 -o 2 -l 16500" (Meyer et al., 2012). We excluded sequences with a mapping quality lower than 25 and removed sequences shorter than 35 bp to avoid spurious alignments from microbial sequences. Finally, we removed PCR duplicates using bam-rmdup (https://github.com/mpieva/biohazard-tools/). We summarize in SOM Table S8 the number of sequences remaining after each step, for each library prepared from extracts of the human tooth. We present in SOM Table S9 the same summary for negative controls prepared at the steps of extraction and library preparation and processed with the same pipeline.

About 38% of the sequences generated from the Riparo Broion tooth carry a cytosine (C) to thymine (T) substitution (in the forward orientation, or guanine [G] to adenine [A] substitution in the reverse orientation) compared to the reference genome within their first three or last three alignment positions (SOM Table S8). Such substitutions mainly stem from the deamination of C bases over time, indicating the preservation of ancient DNA in the specimen (Briggs et al., 2007).

We estimated the proportion of present-day human DNA contamination by counting the number of sequences showing the Neandertal or modern human state at positions that differ between the mitochondrial genomes of 312 present-day humans (Green et al., 2008; including the reference sequence) and 23 Neandertals (Green et al., 2008; Briggs et al., 2009; Gansauge and Meyer, 2014;

Prüfer et al., 2014; Skoglund et al., 2014; Brown et al., 2016; Rougier et al., 2016; Hajdinjak et al., 2018; Peyregne et al., 2019), including the deeply divergent mitochondrial sequence of the Neandertal from Hohlenstein-Stadel Cave. To avoid errors stemming from cytosine deamination, we only looked at sequences in the reverse orientation if one of the diagnostic states was a C, and the forward orientation if one of the diagnostic states was a G. We report the contamination estimates in SOM Table S10.

SOM S3

Reconstruction of the mitochondrial genome

Our preliminary analysis revealed that the mitochondrial genome from the Riparo Broion individual is most similar to the one of Spy 94a (Hajdinjak et al., 2018), a Neandertal found in Spy Cave, Belgium. To minimize the potential effects of reference bias, which may result in a loss of sequences that are too divergent from the rRCS to map to it, we realigned the raw sequences to the mitochondrial sequence of Spy 94a and reprocessed the data as described in the previous section. Summary statistics of this alignment can be found in SOM Table S8.

We then reconstructed the mitochondrial sequence of the Riparo Broion individual. We called a consensus base by a majority vote at every position with at least five overlapping sequences and at least 80% of the sequences carrying the same base. We masked terminal Ts at the three last positions of the sequences before calling the consensus, as they may represent substitutions from ancient DNA damage.

As we estimated that 15% of the sequences aligning to the mitochondrial sequence of Spy 94a represent present-day human DNA contamination (95% binomial confidence interval = 13.5–16.6%; SOM Table S10), we also reconstructed a consensus sequence only using putatively deaminated sequences, i.e., sequences exhibiting C-to-T substitutions within the last three positions of either end. A comparison of the two consensus sequences revealed no differences except in the number of consensus bases that were called.

Some bases in the consensus called using all sequences were unresolved because of a support lower than the 80% cut-off. These likely represent regions where the proportion of present-day

human DNA contamination exceeds 15%. If these bases were resolved in the consensus called using deaminated sequences only, we included them in the final consensus. Only 44 bases remain unresolved. These are found in regions with a low sequence coverage (mainly in the hypervariable region of the mtDNA) that likely reflects an inefficient capture of the endogenous DNA fragments based on the probes designed using a present-day human mitochondrial genome.

SOM S4

Phylogenetic analysis

We used BEAST2 v. 2.6.1 (Bouckaert et al., 2014) to estimate when the individual from Riparo Broion lived and resolve how its mitochondrial genome relates to the ones of present-day and ancient humans. We used the mitochondrial sequence of 23 Neandertals (Green et al., 2008; Briggs et al., 2009; Gansauge and Meyer, 2014; Prüfer et al., 2014; Skoglund et al., 2014; Brown et al., 2016; Rougier et al., 2016; Hajdinjak et al., 2018; Peyrégne et al., 2019), 54 present-day humans (Ingman et al., 2000), 10 early modern humans (Ermini et al., 2008; Gilbert et al., 2008; Krause et al., 2010; Fu et al., 2013a; Fu et al., 2013b; Fu et al., 2014), 4 Denisovans (Krause et al., 2010; Reich et al., 2010; Sawyer et al., 2015; Slon et al., 2017a), a hominin from Sima de los Huesos (Meyer et al., 2014) and a chimpanzee as an outgroup (isolate Jenny, Arnason et al., 1996). For consistency with previous work (Posth et al., 2017; Peyrégne et al., 2019), we restrained our analysis to the mitochondrial sequence outside the hypervariable region (i.e., positions 577-16,023 in rCRS coordinates; Fu et al., 2013b).

To identify the best fitting substitution model, we used jModelTest 2.1.10 (Santorum et al., 2014) and computed several model selection measures (Bayesian information criterion [BIC], a performance measure based on decision theory [DT], and the corrected Akaike information criterion [AICc]). The results of this analysis are reported in SOM Table S11 and the best fitting substitution model is Tamura-Nei 1993 (Tamura and Nei, 1993), according to the BIC and DT measures and ranked second according to the AICc.

We then performed a marginal likelihood estimation analysis to identify the best fitting clock model and tree model. We used the path sampling approach implemented in the

MODEL_SELECTION package (Bouckaert et al., 2014) and tested four model combinations with either a strict clock or uncorrelated lognormal clock and a constant population size or Bayesian Skyline model. We used 40 path steps and a chain length of 25,000,000 iterations for each model combination. To space out steps, we set the parameter alpha of the Beta distribution to 0.3. The pre-burn-in was set to 75,000 iterations followed by a burn-in representing 80% of the chain. We used a mutation rate of 1.57×10-8 substitution per site per year, obtained previously by comparing this region of the mitochondrial genome in present-day and directly radiocarbon-dated early modern humans (Fu et al., 2013b). We fixed the mean mutation rate of the uncorrelated lognormal clock model to the estimate of the human mutation rate reported above and used a gamma distributed standard deviation. The date of modern samples was set to 0 while uniform priors were used for the ancient samples, using either a range spanning the 95% confidence intervals for the dated individuals (see the supplementary information of Posth et al., 2017 and Hajdinjak et al., 2018 for these calibrated radiocarbon dates, with the exception of El Sidrón 1253 for which we used the most recent estimates from Wood et al., 2013) or a range from 30 to 200 ka for the undated Neandertals (initial value of 50 ka) and 30 to 300 ka for the Denisovans (with the exception of Denisova 3, for whom we used a narrower range from 30 to 100 ka to reflect prior knowledge from the analysis of the nuclear genome; Prüfer et al., 2017). For the age of the Sima de los Huesos hominin, we used a uniform prior spanning the confidence intervals of the most recent dates (Arsuaga et al., 2014) from 260 to 780 ka. Finally, we constrained modern humans and Neandertals as two monophyletic groups and set a uniform prior from 50 ka to infinity for the most recent common ancestor of modern humans and from 100 ka to infinity for the most recent common ancestor of Neandertals (excluding the Sima de los Huesos hominin).

The best fitting tree model was the Bayesian Skyline tree model ($\log_{10}$ Bayes factor > 9; SOM Table S12) but there was no significant difference in the fit of the clock models ($\log_{10}$ Bayes Factor = 0.44; SOM Table S12). Therefore, we used the combination of the Bayesian skyline tree model with the simplest model of a fixed molecular clock in three Markov chain Monte Carlo runs of 75,000,000 iterations, sampling parameter values and trees every 5000 iterations, with a burn-in of 15,000,000 iterations. We then merged the results using the program logcombiner (Bouckaert et al., 2014). All estimates with their 95% highest posterior density intervals (HPDI) are reported in SOM Table S13. Based on the length of its branch, we estimate that the individual from Riparo Broion dates to 39 ka (95% HPDI = 30–46 ka), which is in agreement with the archaeological

context. The reconstructed tree (Fig. 7) shows a close relationship between the mtDNA of the Riparo Broion individual and the mtDNA of Neandertals found in Belgium (Spy 94a, Goyet Q305-7, Goyet Q374a-1 and Goyet Q56-1) with a most recent mitochondrial common ancestor 47 ka (95% HPDI: 43–51 ka).

SOM S5

Import presence/absence data on morphological traits across reference and study groups

```
CategoricalPresAbs<-read.csv("SOM_Table_S17.csv",
                             header=T,
                             row.names=1,
                             sep=",")
print(CategoricalPresAbs)
```

```
##            taxon Outline.symmetry Buccal.bulging Mesial.crest
## R_d_Marsal   NEA                1              1            0
## Engis_2      NEA                1              1            1
## LQ_33        NEA                1              1            1
## KRP_D23      NEA                1              1            1
## KMH_22       NEA                1              1            1
## Qafzeh_12    EHS                0              1            1
## Qafzeh_15    EHS                0              0            0
## 1            RHS                0              1            0
## 1b           RHS                0              1            0
## 2b           RHS                1              0            1
## 3a           RHS                1              1            0
## 3b           RHS                1              1            1
## T16          RHS                0              0            0
## T43          RHS                0              0            0
## T48          RHS                0              1            1
## T64          RHS                0              0            1
## T54          RHS                1              1            1
## T53          RHS                1              1            1
## 4            RHS                0              0            1
## T124         RHS                0              0            1
## T76          RHS                1              1            1
## T75          RHS                0              0            1
## T72          RHS                0              0            0
## T71          RHS                0              0            0
```

```
## T70          RHS                0              0              1
## T63          RHS                0              0              1
## T61          RHS                0              0              0
## Broion        BR                1              1              1
```

 # Computing the relative frequency of traits for each group and for Riparo Broion 1

```
CategoricalFreqs<-aggregate(CategoricalPresAbs[,2:4],
                            by=list(CategoricalPresAbs$taxon), FUN=sum)
CategoricalFreqs_rel<-prop.table(as.matrix(CategoricalFreqs[,2:4]),1)
rownames(CategoricalFreqs_rel)<-CategoricalFreqs$Group.1
print(CategoricalFreqs_rel)
```

```
##     Outline.symmetry Buccal.bulging Mesial.crest
## BR         0.3333333      0.3333333    0.3333333
## EHS        0.0000000      0.5000000    0.5000000
## NEA        0.3571429      0.3571429    0.2857143
## RHS        0.2307692      0.3076923    0.4615385
```

SOM S6

Exploring overlap between groups based on relative frequency of morphological traits.

```
CategoricalDist<-(1-sim.table(CategoricalFreqs_rel))
rownames(CategoricalDist)<-rownames(CategoricalFreqs_rel)
colnames(CategoricalDist)<-rownames(CategoricalFreqs_rel)
CategoricalDist<-as.dist(CategoricalDist)
```

```
#  BR           EHS          NEA
# EHS 0.190874505
# NEA 0.001914812 0.208546842
#RHS 0.014624206 0.132613693 0.026264248
```

SOM S7

Calculating means and 95%CIs for Recent *H. sapiens* and Neanderthals

```
# Crown BL diameter
```

```
meanMS<-mean(mdbl_RHS[,3])
CIulMS<-mean(mdbl_RHS[,3])+
  (std.error(mdbl_RHS[,3])*1.96)
CIllMS<-mean(mdbl_RHS[,3])-
  (std.error(mdbl_RHS[,3])*1.96)

meanUPMHS<-mean(mdbl_UPMHS[,3])
CIulUPMHS<-mean(mdbl_UPMHS[,3])+
  (std.error(mdbl_UPMHS[,3])*1.96)
CIllUPMHS<-mean(mdbl_UPMHS[,3])-
  (std.error(mdbl_UPMHS[,3])*1.96)

meanN<-mean(mdbl_NEA[,3])
CIulN<-mean(mdbl_NEA[,3])+
  (std.error(mdbl_NEA[,3])*1.96)
CIllN<-mean(mdbl_NEA[,3])-
  (std.error(mdbl_NEA[,3])*1.96)

c(meanN, CIulN, CIllN)

## [1] 6.862353 7.117328 6.607378

c(meanUPMHS, CIulUPMHS, CIllUPMHS)

## [1] 6.230753 6.326475 6.135030

c(meanMS, CIulMS, CIllMS)

## [1] 6.095500 6.271714 5.919286
```

```
# Cervical BL diameter
meanMS_cervical_BL<-mean(mdbl_noFS_cervical[mdbl_noFS_cervical[,1]=="RHS",3])
CIulMS_cervical_BL<-mean(mdbl_noFS_cervical[mdbl_noFS_cervical[,1]=="RHS",3])+
(std.error(mdbl_noFS_cervical[mdbl_noFS_cervical[,1]=="RHS",3])*1.96)
CIllMS_cervical_BL<-mean(mdbl_noFS_cervical[mdbl_noFS_cervical[,1]=="RHS",3])-
(std.error(mdbl_noFS_cervical[mdbl_noFS_cervical[,1]=="RHS",3])*1.96)

meanN_cervical_BL<-mean(mdbl_noFS_cervical[mdbl_noFS_cervical[,1]=="NEA",3])
CIulN_cervical_BL<-mean(mdbl_noFS_cervical[mdbl_noFS_cervical[,1]=="NEA",3])+
(std.error(mdbl_noFS_cervical[mdbl_noFS_cervical[,1]=="NEA",3])*1.96)
CIllN_cervical_BL<-mean(mdbl_noFS_cervical[mdbl_noFS_cervical[,1]=="NEA",3])-
(std.error(mdbl_noFS_cervical[mdbl_noFS_cervical[,1]=="NEA",3])*1.96)
```

```
c(meanMS_cervical_BL, CIulMS_cervical_BL, CIllMS_cervical_BL)
```

```
## [1] 5.427500 5.592896 5.262104
```

```
c(meanN_cervical_BL, CIulN_cervical_BL, CIllN_cervical_BL)
```

```
## [1] 6.272000 6.555042 5.988958
```

```
# Crown MD diameter
 meanMS_MD<-mean(mdbl_RHS[,2])
CIulMS_MD<-mean(mdbl_RHS[,2])+
  (std.error(mdbl_RHS[,2])*1.96)
CIllMS_MD<-mean(mdbl_RHS[,2])-
  (std.error(mdbl_RHS[,2])*1.96)

meanUPMHS_MD<-mean(mdbl_UPMHS[,2])
CIulUPMHS_MD<-mean(mdbl_UPMHS[,2])+
  (std.error(mdbl_UPMHS[,2])*1.96)
CIllUPMHS_MD<-mean(mdbl_UPMHS[,2])-
  (std.error(mdbl_UPMHS[,2])*1.96)

meanN_MD<-mean(mdbl_NEA[,2])
CIulN_MD<-mean(mdbl_NEA[,2])+
  (std.error(mdbl_NEA[,2])*1.96)
CIllN_MD<-mean(mdbl_NEA[,2])-
  (std.error(mdbl_NEA[,2])*1.96)

c(meanN_MD, CIulN_MD, CIllN_MD)
```

```
## [1] 7.588824 7.884743 7.292904
```

```
c(meanUPMHS_MD, CIulUPMHS_MD, CIllUPMHS_MD)
```

```
## [1] 6.953495 7.049953 6.857036
```

```
c(meanMS_MD, CIulMS_MD, CIllMS_MD)
```

```
## [1] 6.94200 7.14901 6.73499
```

```
# Cervical MD diameter
meanMS_cervical_MD<-mean(mdbl_noFS_cervical[mdbl_noFS_cervical[,1]=="RHS",2])
```

```
CIulMS_cervical_MD<-mean(mdbl_noFS_cervical[mdbl_noFS_cervical[,1]=="RHS",2])+
(std.error(mdbl_noFS_cervical[mdbl_noFS_cervical[,1]=="RHS",2])*1.96)
CIllMS_cervical_MD<-mean(mdbl_noFS_cervical[mdbl_noFS_cervical[,1]=="RHS",2])-
(std.error(mdbl_noFS_cervical[mdbl_noFS_cervical[,1]=="RHS",2])*1.96)

meanN_cervical_MD<-mean(mdbl_noFS_cervical[mdbl_noFS_cervical[,1]=="NEA",2])
CIulN_cervical_MD<-mean(mdbl_noFS_cervical[mdbl_noFS_cervical[,1]=="NEA",2])+
(std.error(mdbl_noFS_cervical[mdbl_noFS_cervical[,1]=="NEA",2])*1.96)
CIllN_cervical_MD<-mean(mdbl_noFS_cervical[mdbl_noFS_cervical[,1]=="NEA",2])-
(std.error(mdbl_noFS_cervical[mdbl_noFS_cervical[,1]=="NEA",2])*1.96)

c(meanMS_cervical_MD, CIulMS_cervical_MD, CIllMS_cervical_MD)

## [1] 5.28900 5.47299 5.10501

c(meanN_cervical_MD, CIulN_cervical_MD, CIllN_cervical_MD)

## [1] 6.044000 6.345267 5.742733
```

SOM S8

All the following sections present with R codes and printing of analysis results to facilitate reproducibility. Relevant packages can be downloaded from R. Source codes can be downloaded as supplementary data files from the online publication website.

```
# run in R version 3.4.4 on Linux
# Rmarkdown file compiled in RStudio desktop version 1.2.5

source("SOM_File_1.R")
source("SOM_File_2.R")
source("SOM_File_3.R")
library(plotrix)
library(effsize)
library(pwr)
library(vegetarian)
```

Import values of MD and BL diameter for all sampled individuals. Each specimen is attributed to a taxon, namely NEA=Neanderthal (n=5), EHS=Early *H. sapiens* (n=2), UPHS=Upper Palaeolithic *H. sapiens*, RHS=Recent *H. sapiens* (n=20).

```
mdbl<-read.csv("SOM_Table_S15.csv", header=T,row.names=1, sep=",")
```

```
mdbl_cervical<-read.csv("SOM_Table_S18.csv", header=T,row.names=1, sep=",")
```

The presence of significant differences among groups is tested through a non parametric Kruskal-Wallis test and via pairwise post-hoc Mann-Whitney tests using the original attached source code "SOM_FileS1.R". The first section of results reports statistics for Kruskal-Wallis test, while the second section reports Mann-Whitney p-values in the first element of listed results (indicated by number [[1]]), and Bonferroni corrected p-values in the second element of listed results (indicated by number [[2]]).

```
# Testing for differences among groups

# Crown BL diameter

explore(mdbl,3,1)
```

```
##
## Kruskal-Wallis rank sum test
##
## data:  data[, colvar1] by data[, colvar2]
## Kruskal-Wallis chi-squared = 25.97, df = 3, p-value = 9.676e-06
```

```
## [[1]]
##          EHS    NEA    RHS
## NEA   0.4632
## RHS   0.0258 0.0001
## UPMHS 0.0323 0.0000 0.2558
##
## [[2]]
## [1] 1.0000 0.1548 0.1938 0.0006 0.0000 1.0000
```

```
# Cervical BL diameter
```

```
explore(mdbl_cervical,3,1)
```

```
##
## Kruskal-Wallis rank sum test
##
## data:  data[, colvar1] by data[, colvar2]
## Kruskal-Wallis chi-squared = 13.202, df = 3, p-value = 0.00422
```

```
## [[1]]
##         EHS    NEA    RHS
## NEA  0.1752
## RHS  0.0865 0.0018
## UPHS 0.2453 0.0814 0.4577
##
## [[2]]
## [1] 1.0000 0.5190 1.0000 0.0108 0.4884 1.0000
```

```
# Crown MD diameter
```

```
explore(mdbl,2,1)
```

```
##
## Kruskal-Wallis rank sum test
##
## data:  data[, colvar1] by data[, colvar2]
## Kruskal-Wallis chi-squared = 21.812, df = 3, p-value = 7.136e-05
```

```
## [[1]]
##          EHS    NEA    RHS
## NEA   0.0967
## RHS   0.0259 0.0012
## UPMHS 0.0176 0.0001 0.9161
##
## [[2]]
## [1] 0.5802 0.1554 0.1056 0.0072 0.0006 1.0000
```

```
# Cervical MD diameter
```

```
explore(mdbl_cervical,2,1)
```

```
##
## Kruskal-Wallis rank sum test
##
## data:  data[, colvar1] by data[, colvar2]
## Kruskal-Wallis chi-squared = 12.628, df = 3, p-value = 0.005513

## [[1]]
##         EHS    NEA    RHS
## NEA  0.8465
## RHS  0.0456 0.0028
## UPHS 0.2453 0.0814 0.7317
##
## [[2]]
## [1] 1.0000 0.2736 1.0000 0.0168 0.4884 1.0000
```

SOM S9

EHS specimens are discarded in order to directly compare Upper Palaeolithic *H. sapiens*, Mesolithic *H. sapiens*, Recent *H. sapiens* and Neanderthals.

```
#crown measures
mdbl_NEA_UPMHS<-subset(mdbl, taxon=="NEA"|taxon=="UPMHS")
mdbl_NEA_UPMHS<-droplevels(mdbl_NEA_UPMHS)
mdbl_NEA_RHS<-subset(mdbl, taxon=="NEA"|taxon=="RHS")
mdbl_NEA_RHS<-droplevels(mdbl_NEA_RHS)

mdbl_NEA<-subset(mdbl, taxon=="NEA")
mdbl_NEA<-droplevels(mdbl_NEA)

mdbl_RHS<-subset(mdbl, taxon=="RHS")
mdbl_RHS<-droplevels(mdbl_RHS)

mdbl_UPMHS<-subset(mdbl, taxon=="UPMHS")
mdbl_UPMHS<-droplevels(mdbl_UPMHS)

#cervical measures

mdbl_noFS_cervical<-
mdbl_cervical[mdbl_cervical[,1]=="RHS"|mdbl_cervical[,1]=="NEA",]
mdbl_noFS_cervical<-droplevels(mdbl_noFS_cervical)
print(mdbl_noFS_cervical)
```

Effect size for difference in means between Recent *H. sapiens* and Neanderthals

```
# Crown BL diameter

#NEA/UPMHS
cohen.d(d=mdbl_NEA_UPMHS[,3], f=mdbl_NEA_UPMHS[,1], pooled=T,
        paired=F, hedges.correction=T,conf.level=.95)

##
## Hedges's g
##
## g estimate: 1.303348 (large)
## 95 percent confidence interval:
##     lower     upper
## 0.7560908 1.8506048



#NEA/RHS
cohen.d(d=mdbl_NEA_RHS[,3], f=mdbl_NEA_RHS[,1], pooled=T,
        paired=F, hedges.correction=T,conf.level=.95)

##
## Hedges's g
##
## g estimate: 1.602294 (large)
## 95 percent confidence interval:
##     lower     upper
## 0.8498134 2.3547754




# Cervical BL diameter

cohen.d(d=mdbl_noFS_cervical[,3], f=mdbl_noFS_cervical[,1], pooled=T,
        paired=F, hedges.correction=T,conf.level=.95)

##
## Hedges's g
##
## g estimate: 2.216231 (large)
## 95 percent confidence interval:
```

```
##    lower    upper
## 1.035733 3.396729
```

```
# Crown MD diameter
```

```
#NEA/UPMHS
cohen.d(d=mdbl_NEA_UPMHS[,2], f=mdbl_NEA_UPMHS[,1], pooled=T,
        paired=F, hedges.correction=T,conf.level=.95)
```

```
##
## Hedges's g
##
## g estimate: 1.263629 (large)
## 95 percent confidence interval:
##    lower    upper
## 0.718015 1.809243
```

```
#NEA/RHS
cohen.d(d=mdbl_NEA_RHS[,2], f=mdbl_NEA_RHS[,1], pooled=T,
        paired=F, hedges.correction=T,conf.level=.95)
```

```
##
## Hedges's g
##
## g estimate: 1.158811 (large)
## 95 percent confidence interval:
##     lower     upper
## 0.4510379 1.8665835
```

```
# Cervical MD diameter
```

```
cohen.d(d=mdbl_noFS_cervical[,2], f=mdbl_noFS_cervical[,1], pooled=T,
        paired=F, hedges.correction=T,conf.level=.95)
```

```
##
## Hedges's g
##
## g estimate: 1.791257 (large)
## 95 percent confidence interval:
##     lower     upper
## 0.6699783 2.9125361
```

SOM S10

Measuring power

To further support previous results we measure statistical power for an unpaired t-test with unequal sample size based on previously calculated effect size and given significance level.

```
#Crown BL diameter
#NEA/UPMHS
pwr.t2n.test(n1=17,n2=93, d=1.303348, sig.level=0.05)
```

```
##
##      t test power calculation
##
##              n1 = 17
##              n2 = 93
##               d = 1.303348
##       sig.level = 0.05
##           power = 0.9983421
##     alternative = two.sided
```

```
#NEA/RHS
pwr.t2n.test(n1=17,n2=20, d=1.602294, sig.level=0.05)
```

```
##
##      t test power calculation
##
##              n1 = 17
##              n2 = 20
##               d = 1.602294
##       sig.level = 0.05
##           power = 0.9971114
##     alternative = two.sided
```

```
#Cervical BL diameter
pwr.t2n.test(n1=5,n2=20, d=2.216231, sig.level=0.05)
```

```
##
##      t test power calculation
##
##              n1 = 5
```

```
##              n2 = 20
##               d = 2.216231
##       sig.level = 0.05
##           power = 0.9887212
##     alternative = two.sided
```

```
#Crown MD diameter
#NEA/UPMHS
pwr.t2n.test(n1=17,n2=93, d=1.263629, sig.level=0.05)
```

```
##
##      t test power calculation
##
##              n1 = 17
##              n2 = 93
##               d = 1.263629
##       sig.level = 0.05
##           power = 0.9973453
##     alternative = two.sided
```

```
#NEA/RHS
pwr.t2n.test(n1=17,n2=20, d=1.158811, sig.level=0.05)
```

```
##
##      t test power calculation
##
##              n1 = 17
##              n2 = 20
##               d = 1.158811
##       sig.level = 0.05
##           power = 0.927152
##     alternative = two.sided
```

```
#Cervical MD diameter
pwr.t2n.test(n1=5,n2=20, d=1.791257, sig.level=0.05)
```

```
##
##      t test power calculation
##
```

```
##              n1 = 5
##              n2 = 20
##               d = 1.791257
##       sig.level = 0.05
##           power = 0.9291329
##     alternative = two.sided
```

SOM S11

Testing if BL and MD diameters in Neanderthals, Upper Palaeolithic, Mesolithic, and Recent *H. sapiens* are normally distributed via Shapiro-Wilk tests

```
# Crown BL diameter

# NEA
shapiro.test(mdbl_NEA[,3])
```

```
##
## Shapiro-Wilk normality test
##
## data:  mdbl_NEA[, 3]
## W = 0.81819, p-value = 0.003642
```

```
# UPMHS

shapiro.test(mdbl_UPMHS[,3])
```

```
##
## Shapiro-Wilk normality test
##
## data:  mdbl_UPMHS[, 3]
## W = 0.98695, p-value = 0.4878
```

```
# RHS
```

```
##
## Shapiro-Wilk normality test
##
```

```
## data:  mdbl_RHS[, 3]
## W = 0.93475, p-value = 0.1905
```

```
# Cervical BL diameter
shapiro.test(mdbl_noFS_cervical[mdbl_noFS_cervical[,1]=="RHS",3])
```

```
##
## Shapiro-Wilk normality test
##
## data:  mdbl_noFS_cervical[mdbl_noFS_cervical[, 1] == "RHS", 3]
## W = 0.91578, p-value = 0.08221
```

```
# Crown MD diameter
# NEA
```

```
shapiro.test(mdbl_NEA[,2])
```

```
##
## Shapiro-Wilk normality test
##
## data:  mdbl_NEA[, 2]
## W = 0.95396, p-value = 0.522
```

```
# UPMHS
```

```
shapiro.test(mdbl_UPMHS[,2])
```

```
##
## Shapiro-Wilk normality test
##
## data:  mdbl_UPMHS[, 2]
## W = 0.97649, p-value = 0.09147
```

```
# RHS
```

```
shapiro.test(mdbl_RHS[,2])
```

```
##
## Shapiro-Wilk normality test
##
```

```
## data:  mdbl_RHS[, 2]
## W = 0.88494, p-value = 0.02174
```

```
# Cervical MD diameter
shapiro.test(mdbl_noFS_cervical[mdbl_noFS_cervical[,1]=="RHS",2])
```

```
##
## Shapiro-Wilk normality test
##
## data:  mdbl_noFS_cervical[mdbl_noFS_cervical[, 1] == "RHS", 2]
## W = 0.98495, p-value = 0.9813
```

SOM S12

One-tailed t-test for comparison of a single observation (Riparo Broion 1) with the mean of a sample (Recent *H. sapiens*)

```
# Crown BL diameter
```

```
ttest1ob(6.84,mdbl_UPMHS[,3])
```

```
## [1] "Test Statistic"
## [1] 1.286685
## [1] "p of obtaining a more extreme value"
## [1] 0.1007161
## [1] "Df"
## [1] 92
```

```
ttest1ob(6.84,mdbl_RHS[,3])
```

```
## [1] "Test Statistic"
## [1] 1.807057
## [1] "p of obtaining a more extreme value"
## [1] 0.04330797
## [1] "Df"
## [1] 19
```

```
# Cervical BL diameter
```

```
ttest1ob(6.22,mdbl_noFS_cervical[mdbl_noFS_cervical[,1]=="RHS",3])
```

```
## [1] "Test Statistic"
## [1] 2.049366
## [1] "p of obtaining a more extreme value"
## [1] 0.02724503
## [1] "Df"
## [1] 19
```

```
# Cervical MD diameter
```

```
ttest1ob(6.23,mdbl_noFS_cervical[mdbl_noFS_cervical[,1]=="RHS",2])
```

```
## [1] "Test Statistic"
## [1] 2.187467
## [1] "p of obtaining a more extreme value"
## [1] 0.02070669
## [1] "Df"
## [1] 19
```

SOM S13

Exploring differences between Neanderthal and Recent *H. sapiens* in Coronal pulp Index elaborated in the present work

```
indices<-read.csv("SOM_Table_S16.csv", header=T, sep=",", row.names=1)

wilcox.test(indices[indices$taxon=="NEA",3],
            indices[indices$taxon=="RHS",3],
            paired=F, exact=T)
##
## Wilcoxon rank sum test
##
## data:  indices[indices$taxon == "NEA", 3] and indices[indices$taxon ==
"RHS", 3]
## W = 34, p-value = 0.3027
## alternative hypothesis: true location shift is not equal to 0
```

SOM S14

Exploring differences between Neanderthal and Recent *H. sapiens* in 3D Lateral RET

```r
wilcox.test(indices[indices$taxon=="NEA",7],
            indices[indices$taxon=="RHS",7],
            paired=F, exact=T)
```

```
##
## Wilcoxon rank sum test
##
## data:  indices[indices$taxon == "NEA", 7] and indices[indices$taxon ==
"RHS", 7]
## W = 25, p-value = 0.09697
## alternative hypothesis: true location shift is not equal to 0
```

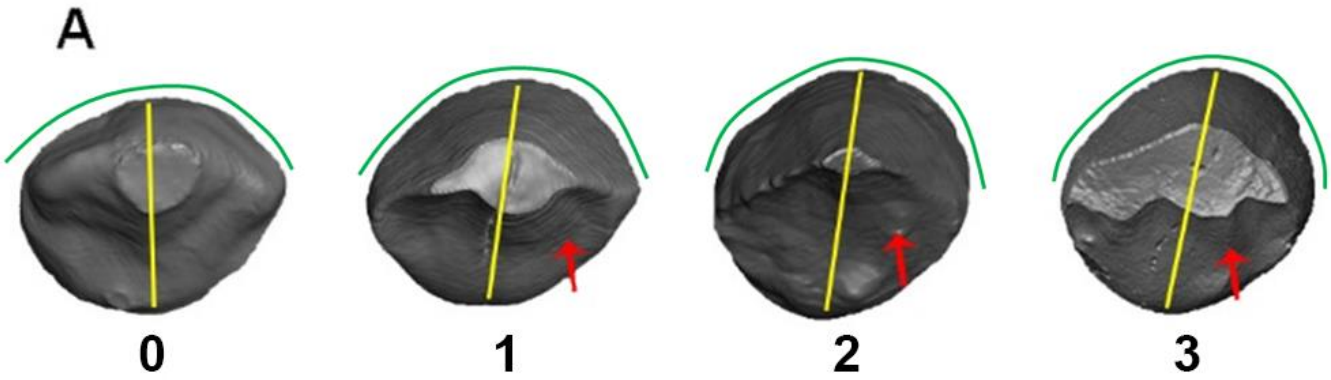

SOM Figure S1. Four degrees of expression of the three morphological features: buccal bulging (green curve), asymmetry of EDJ outline (yellow line) and mesial crest (pointed by the red arrow).

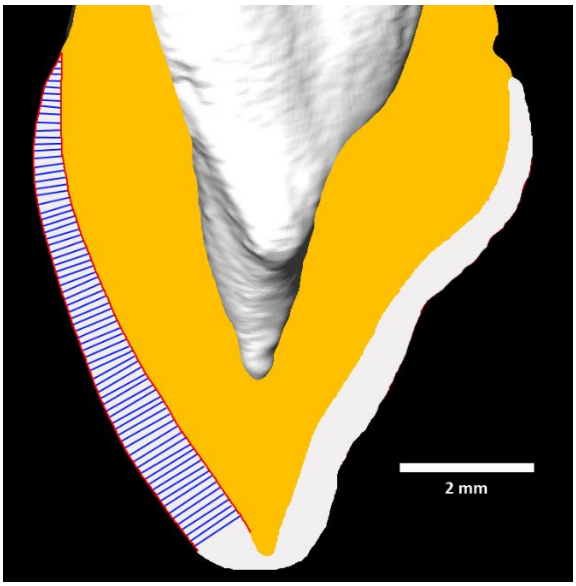

SOM Figure S2. Bidimensional topographic variation of enamel thicknesses measured on the buccal aspect of the sample RHS 48.

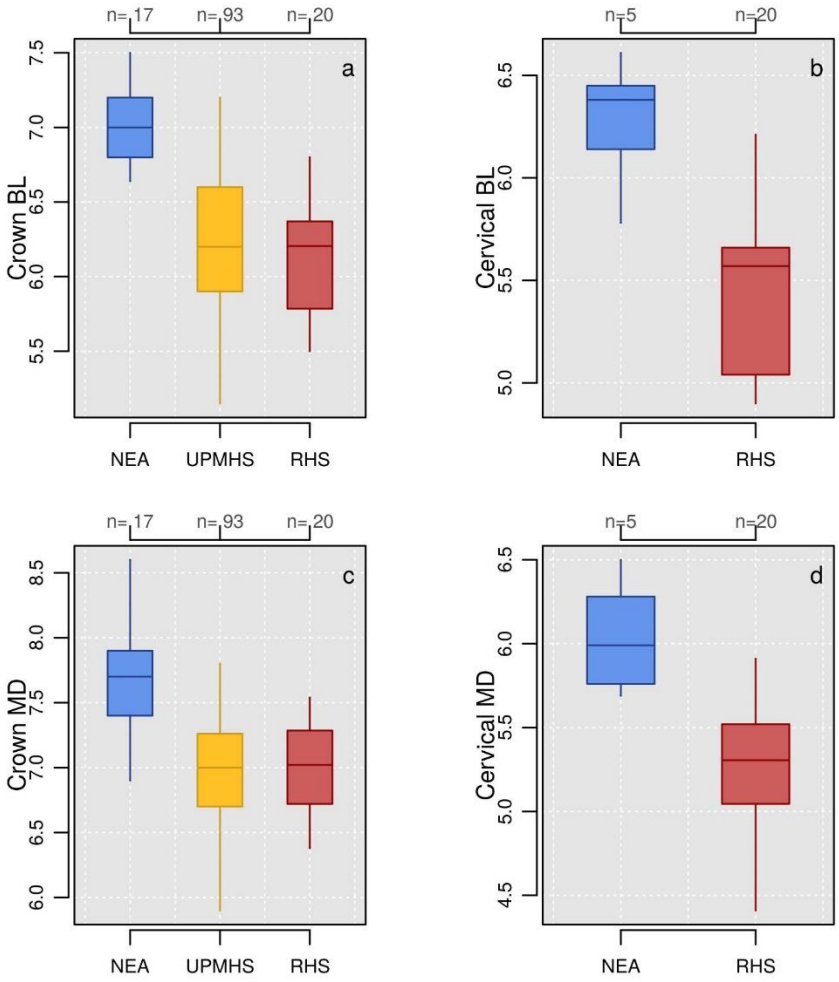

SOM Figure S3. Boxplot showing the distribution of buccolingual crown diameter (CrownBL), buccolingual cervical diameter (CervicalBL), mesiodistal crown diameter (CrownMD), and mesiodistal cervical diameter (CervicalMD) in Neanderthals (blue), Upper Paleolithic and Mesolithic *H. sapiens* (yellow), and recent *H. sapiens* (red) .

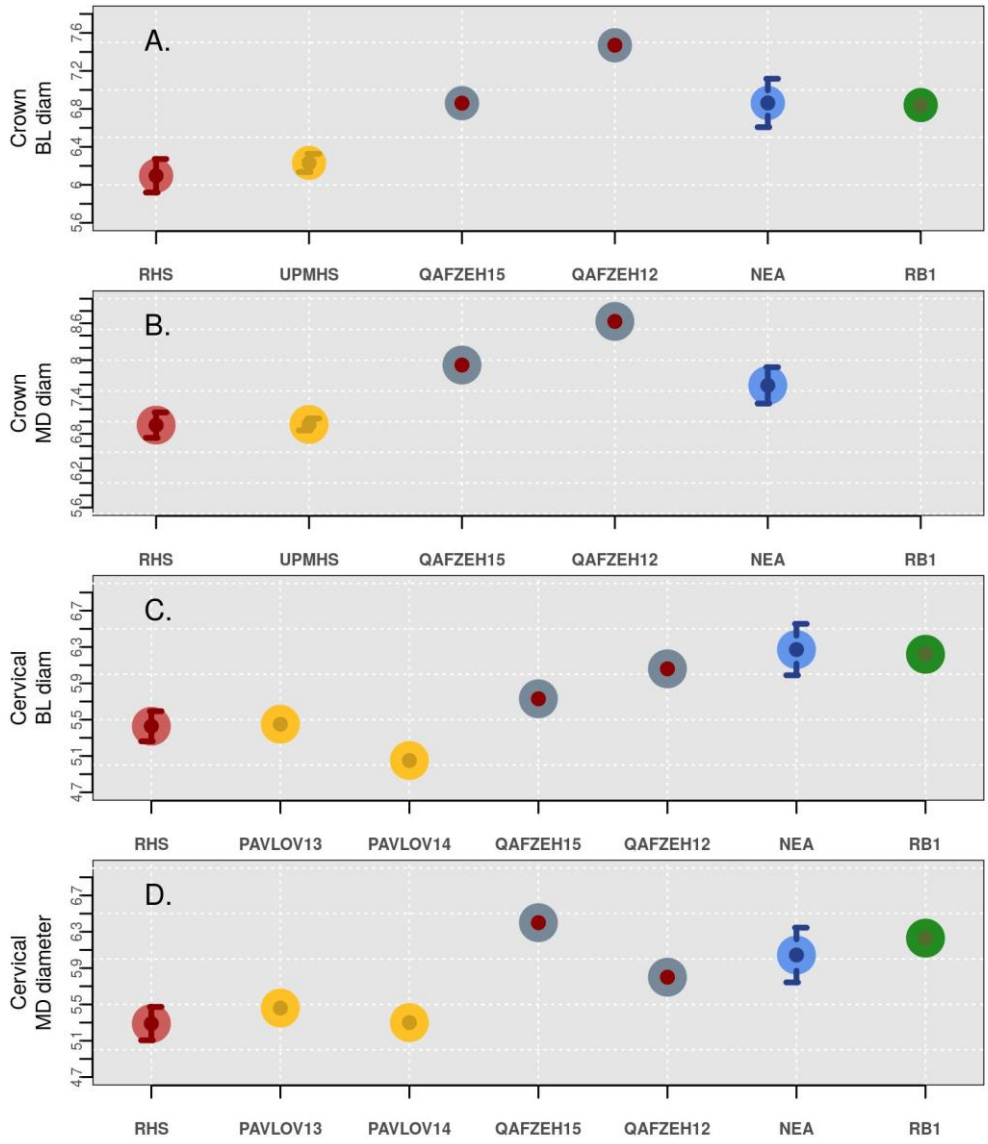

SOM Figure S4. Mean values and 95% CIs for recent *Homo sapiens,* Upper Paleolithic/Mesolithic *H. sapiens* and Neanderthals plotted against individual values for early *H. sapiens* (gray dots) and Riparo Broion 1 (green dot, where available). Only individual point estimates of Upper Paleolithic *H. sapiens* (Pavlov13 and Pavlov14; yellow dots) are available for cervical values. A) Buccolingual crown diameter. B) Buccolingual cervical diameter. C) Mesiodistal crown diameter. D) Mesiodistal cervical diameter.

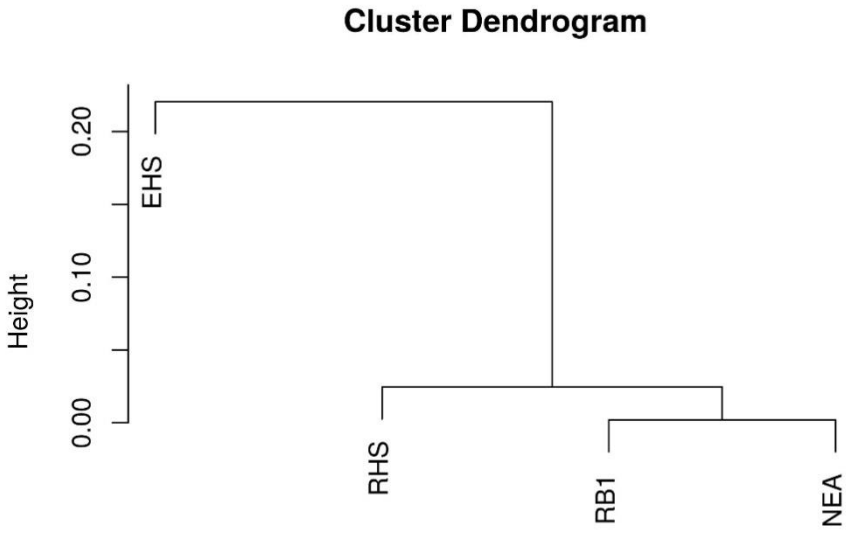

SOM Figure S5. Hierarchical clustering based on the inverse of the overlap in the relative frequency of morphological traits among Neanderthals (NEA), recent *Homo sapiens* (RHS), early *H. sapiens* (EHS), and Riparo Broion 1 (RB1).

SOM Table S1

Comparison sample of human fossils.

Taxon	Sample	Ind#	Wear stage	Side	Reference
NEA	Valdegoba	2	not specified	L	Voisin et al. (2012)
NEA	Dederiyeh	1	not specified	R	Voisin et al. (2012)
NEA	Krapina	D23	3[a]	L	this study
NEA	Krapina	7	not specified	L	Frayer (1978)
NEA	Krapina	7	not specified	R	Frayer (1978)
NEA	Pinar	7	not specified	L	Voisin et al. (2012)
NEA	Roc de Marsal	a	2[a]	L	Voisin et al. (2012)
NEA	Roc de Marsal	b	no wear	R	this study
NEA	Subaluk	2	not specified	L	Voisin et al. (2012)
NEA	Subaluk	2	not specified	R	Voisin et al. (2012)
NEA	Engis	2	3[a]	L	this study
NEA	La Quina	33	4[a]	R	this study
NEA	Kebara	22	4[a]	L	this study
NEA	Portel-Ouest Cave	LP_20	6[a]	R	Becam and Chevalier (2019)
NEA	Portel-Ouest Cave	LP_23	6[a]	L	Becam and Chevalier (2019)
NEA	Beau de l'Aubesier6	Aubesier 6	3[a]	L	Voisin et al. (2012)
NEA	Grotte du Bison (Arcy sur Cure)	O11-192	not specified	L	Voisin et al. (2012)
NEA	Grotte du Renne (Arcy-sur-Cure)	37	1[b]	L	Frayer (1978)
NEA	Grotte du Renne (Arcy-sur-Cure)	38	0[b]	L	Frayer (1978)
EHS	Qafzeh	15	4[a]	R	This study
EHS	Qafzeh	12	4[a]	R	This study
UPMHS	Fourneau du Diable	900	not specified	R	Frayer (1978)
UPMHS	Pavlov13	900	5[a]	R	This study
UPMHS	Pavlov14	903	5[a]	R	This study
UPMHS	Pavlov	908	not specified	L	Frayer (1978)
UPMHS	Pavlov	909	not specified	L	Frayer (1978)
UPMHS	La Madeleine	IV	not specified	R	Frayer (1978)
UPMHS	St. Germain La Rivière	8	not specified	R	Frayer (1978)

UPMHS	Aveline's Hole	M1.11.242	not specified	L	Frayer (1978)
UPMHS	Rochereil	3	not specified	R	Frayer (1978)
UPMHS	El Cingle Vermell	K8.T7	not specified	L	Frayer (1978)
UPMHS	Ofnet	103,7201389	not specified	R	Frayer (1978)
UPMHS	Ofnet	103,8048611	not specified	L	Frayer (1978)
UPMHS	Ofnet	104,1861111	not specified	L	Frayer (1978)
UPMHS	Ofnet	104,2708333	not specified	R	Frayer (1978)
UPMHS	Ofnet	104,3979167	not specified	R	Frayer (1978)
UPMHS	Felsstalle Muhlen	900	not specified	L	Frayer (1978)
UPMHS	Arene Candide (Epi-Grav.)	11	not specified	L	Frayer (1978)
UPMHS	Arene Candide (Epi-Grav.)	8	not specified	L	Frayer (1978)
UPMHS	Hoedic	7b	not specified	L	Frayer (1978)
UPMHS	Muge Arruda	1.1937.P	not specified	R	Frayer (1978)
UPMHS	Muge Arruda	176c.L	not specified	L	Frayer (1978)
UPMHS	Muge Arruda	901.P	not specified	L	Frayer (1978)
UPMHS	Muge Arruda	916.L	not specified	L	Frayer (1978)
UPMHS	Skateholm2	XIII	not specified	L	Frayer (1978)
UPMHS	Vlasac (Ia + Ib)	53	not specified	L	Frayer (1978)
UPMHS	Obristvi	0,118055556	not specified	R	Frayer (1978)
UPMHS	Obristvi	0,201388889	not specified	R	Frayer (1978)
UPMHS	Krskany	0,586111111	not specified	L	Frayer (1978)
UPMHS	Krskany	28.65	not specified	L	Frayer (1978)
UPMHS	Krskany	30.65	not specified	L	Frayer (1978)
UPMHS	Krskany	38.65	not specified	L	Frayer (1978)
UPMHS	Krskany	50.65	not specified	R	Frayer (1978)
UPMHS	Krskany	60.65	not specified	L	Frayer (1978)
UPMHS	Krskany	67.65	not specified	R	Frayer (1978)
UPMHS	Krskany	68.65	not specified	L	Frayer (1978)

UPMHS	Vedrovice	0,802083333	not specified	R	Frayer (1978)
UPMHS	Vedrovice	0,170833333	not specified	L	Frayer (1978)
UPMHS	Vedrovice	0,214583333	not specified	L	Frayer (1978)
UPMHS	Vedrovice	84.80	not specified	R	Frayer (1978)
UPMHS	Szegvar-Tzkoves	71.27.23.62	not specified	R	Frayer (1978)
UPMHS	Szany	10181	not specified	R	Frayer (1978)
UPMHS	Zalavar-Var	8802	not specified	L	Frayer (1978)
UPMHS	Keszthely	13.80.2.8	not specified	L	Frayer (1978)
UPMHS	Tiszafüred-Mojores	68.133.32.0D49	not specified	L	Frayer (1978)
UPMHS	BP Wekerle-Telep	9563	not specified	L	Frayer (1978)
UPMHS	Budapest-Timur ut	1988.IV.12 16.2	not specified	R	Frayer (1978)
UPMHS	Tiszalök	82.1.101	not specified	L	Frayer (1978)
UPMHS	Pilismar—t	9386	not specified	L	Frayer (1978)
UPMHS	Grotte des Enfants	1	not specified	L	Voisin et al. (2012)
UPMHS	Grotte des Enfants	2	not specified	L	Voisin et al. (2012)
UPMHS	Grotte des Enfants	2	not specified	R	Voisin et al. (2012)
UPMHS	La Geniere	1	not specified	L	Frayer (1978)
UPMHS	La Geniere	1	not specified	R	Frayer (1978)
UPMHS	Hohlenstein	3	not specified	L	Frayer (1978)
UPMHS	Hohlenstein	3	not specified	R	Frayer (1978)
UPMHS	Ofnet	103,0840278	not specified	L	Frayer (1978)
UPMHS	Ofnet	103,0840278	not specified	R	Frayer (1978)
UPMHS	Ofnet	103,2958333	not specified	L	Frayer (1978)
UPMHS	Ofnet	103,2958333	not specified	R	Frayer (1978)
UPMHS	Ofnet	103,3381944	not specified	L	Frayer (1978)
UPMHS	Ofnet	103,3381944	not specified	R	Frayer (1978)
UPMHS	Ofnet	2484.11A	not specified	L	Frayer (1978)
UPMHS	Ofnet	2484.11A	not specified	R	Frayer (1978)

UPMHS	Ofnet	103,55	not specified	L	Frayer (1978)
UPMHS	Ofnet	103,55	not specified	R	Frayer (1978)
UPMHS	Ofnet	103,8472222	not specified	L	Frayer (1978)
UPMHS	Ofnet	103,8472222	not specified	R	Frayer (1978)
UPMHS	Ofnet	103,9319444	not specified	L	Frayer (1978)
UPMHS	Ofnet	103,9319444	not specified	R	Frayer (1978)
UPMHS	Ofnet	103,9743056	not specified	L	Frayer (1978)
UPMHS	Ofnet	103,9743056	not specified	R	Frayer (1978)
UPMHS	Schnellnecker Wand	2	not specified	L	Frayer (1978)
UPMHS	Schnellnecker Wand	2	not specified	R	Frayer (1978)
UPMHS	Arene Candide (Epi-Grav.)	6	not specified	L	Frayer (1978)
UPMHS	Arene Candide (Epi-Grav.)	6	not specified	R	Frayer (1978)
UPMHS	Muge Arruda	4.P	not specified	L	Frayer (1978)
UPMHS	Muge Arruda	4.P	not specified	R	Frayer (1978)
UPMHS	Muge Arruda	48.L	not specified	L	Frayer (1978)
UPMHS	Muge Arruda	48.L	not specified	R	Frayer (1978)
UPMHS	Muge Arruda	917.L	not specified	L	Frayer (1978)
UPMHS	Muge Arruda	917.L	not specified	R	Frayer (1978)
UPMHS	Obristvi	0,079861111	not specified	L	Frayer (1978)
UPMHS	Obristvi	0,079861111	not specified	R	Frayer (1978)
UPMHS	Obristvi	0,159722222	not specified	L	Frayer (1978)
UPMHS	Obristvi	0,159722222	not specified	R	Frayer (1978)
UPMHS	Krskany	13a.64	not specified	L	Frayer (1978)
UPMHS	Krskany	13a.64	not specified	R	Frayer (1978)
UPMHS	Krskany	40.65.1	not specified	L	Frayer (1978)
UPMHS	Krskany	40.65.1	not specified	R	Frayer (1978)
UPMHS	Krskany	49.65	not specified	L	Frayer (1978)
UPMHS	Krskany	49.65	not specified	R	Frayer (1978)

UPMHS	Krskany	54.65	not specified	L	Frayer (1978)
UPMHS	Krskany	54.65	not specified	R	Frayer (1978)
UPMHS	Krskany	71.65	not specified	L	Frayer (1978)
UPMHS	Krskany	71.65	not specified	R	Frayer (1978)
UPMHS	Krskany	74.65	not specified	L	Frayer (1978)
UPMHS	Krskany	74.65	not specified	R	Frayer (1978)
UPMHS	Vedrovice	109.84	not specified	L	Frayer (1978)
UPMHS	Vedrovice	109.84	not specified	R	Frayer (1978)
UPMHS	Vedrovice	0,71875	not specified	L	Frayer (1978)
UPMHS	Vedrovice	0,71875	not specified	R	Frayer (1978)
UPMHS	Vedrovice	0,885416667	not specified	L	Frayer (1978)
UPMHS	Vedrovice	0,885416667	not specified	R	Frayer (1978)
UPMHS	Vedrovice	28.76	not specified	L	Frayer (1978)
UPMHS	Vedrovice	28.76	not specified	R	Frayer (1978)
UPMHS	Vedrovice	39.76	not specified	L	Frayer (1978)
UPMHS	Vedrovice	39.76	not specified	R	Frayer (1978)
UPMHS	Vedrovice	40.76	not specified	L	Frayer (1978)
UPMHS	Vedrovice	40.76	not specified	R	Frayer (1978)
UPMHS	Vedrovice	0,269444444	not specified	L	Frayer (1978)
UPMHS	Vedrovice	0,269444444	not specified	R	Frayer (1978)
UPMHS	Vedrovice	78.79	not specified	L	Frayer (1978)
UPMHS	Vedrovice	78.79	not specified	R	Frayer (1978)
UPMHS	Szegvar-Tzkoves	71.27.11.47	not specified	L	Frayer (1978)
UPMHS	Szegvar-Tzkoves	71.27.11.47	not specified	R	Frayer (1978)
UPMHS	Keszthely	13.80.3.12	not specified	L	Frayer (1978)
UPMHS	Keszthely	13.80.3.12	not specified	R	Frayer (1978)
UPMHS	BP Wekerle-Telep	9551	not specified	L	Frayer (1978)
UPMHS	BP Wekerle-Telep	9551	not specified	R	Frayer (1978)

UPMHS	Tiszfüred	79.5.102.111	not specified	L	Frayer (1978)
UPMHS	Tiszfüred	79.5.102.111	not specified	R	Frayer (1978)
UPMHS	Tiszfüred -Honfoglalaskor	79.5.108.117	not specified	L	Frayer (1978)
UPMHS	Tiszfüred -Honfoglalaskor	79.5.108.117	not specified	R	Frayer (1978)
UPMHS	Tiszfüred -Honfoglalaskor	79.5.16.17	not specified	L	Frayer (1978)
UPMHS	Tiszfüred -Honfoglalaskor	79.5.16.17	not specified	R	Frayer (1978)
UPMHS	Csontuz	2.79.8.23	not specified	L	Frayer (1978)
UPMHS	Csontuz	2.79.8.23	not specified	R	Frayer (1978)
UPMHS	Tiszalök	82.1.176	not specified	L	Frayer (1978)
UPMHS	Tiszalök	82.1.176	not specified	R	Frayer (1978)
UPMHS	Tiszalök	3,417453704	not specified	L	Frayer (1978)
UPMHS	Tiszalök	3,417453704	not specified	R	Frayer (1978)
UPMHS	Nyarsapat	9327	not specified	L	Frayer (1978)
UPMHS	Nyarsapat	9327	not specified	R	Frayer (1978)
UPMHS	Nyarsapat	9345	not specified	L	Frayer (1978)
UPMHS	Nyarsapat	9345	not specified	R	Frayer (1978)
UPMHS	Abri Pataud	P6 (AP/58-2-F2283)	3[c]	R	Voisin et al. (2012)
RHS	T64	T64	3[a]	L	This study
RHS	T43	T43	3[a]	R	This study
RHS	T16	T16	2[a]	L	This study
RHS	3b	3b	4[a]	R	This study
RHS	3a	3a	3[a]	L	This study
RHS	2b	2b	4[a]	R	This study
RHS	1b	1b	4[a]	R	This study
RHS	1	1	4[a]	R	This study
RHS	T54	T54	4[a]	R	This study
RHS	T53	T53	3[a]	R	This study
RHS	4	4	3[a]	R	This study
RHS	T124	T124	4[a]	R	This study
RHS	T76	T76	4[a]	R	This study

RHS	T75	T75	3[a]	R	This study
RHS	T72	T72	3[a]	R	This study
RHS	T71	T71	3[a]	R	This study
RHS	T70	T70	3[a]	R	This study
RHS	T63	T63	2[a]	R	This study
RHS	T61	T61	3[a]	R	This study
RHS	T48	T48	2[a]	L	This study

Abbreviations: L = left; R = right; NEA = Neanderthals; EHS = early *Homo sapiens*; UPMHS = Upper Paleolithic and Mesolithic *H. sapiens* (UPMHS); RHS = recent *H. sapiens* (taken from contemporary individuals from Italy); Ind# = ID code.

Molnar (1971).

[b] Turner et al. (1991).

[c] Smith (1984).

SOM Table S2

Degree of morphological traits observed in each individual (0 = absent, 1 = slight, 2 = evident, 3 = marked).

ID	Outline asymmetry	Buccal bulging	mesial crest
Riparo Broion1	3	2	3
Neanderthals			
Roc de Marsal	1	2	0
Engis2	2	3	2
LQ33	2	3	3
KRPD23	3	3	1
KMH22	2	2	2
Early *Homo sapiens*			
Qafzeh12	0	1	1
Qafzeh15	0	0	0
Recent *Homo sapiens*			
1	0	1	0
1b	0	1	0
2b	1	0	1
3a	1	1	0
3b	1	1	1
T16	0	0	0
T43	0	0	0
T48	0	1	3
T64	0	0	3
T54	1	2	1
T53	1	1	1
4	0	0	1
T124	0	0	1
T76	1	1	1
T75	0	0	1
T72	0	0	0
T71	0	0	0
T70	0	0	1
T63	0	0	1
T61	0	0	0

SOM Table S3
Dental crown dimensions of the comparative sample and Riparo Broion 1.

						Mean	
Site	ind#	Wear	Side	MD	BL	MD	BL
Riparo Broion	1	4[a]	R	N.A.	6.84		
Valdegoba	2	not specified	L	6.60	5.80		
Dederiyeh	1	not specified	R	7.80	7.30		
Krapina	D23	3[a]	L	8.38	7.30		
Krapina	7	not specified	L	8.4	6.6	8.2	6.8
Krapina	7	not specified	R	8	6.9		
Pinar	7	not specified	L	7.90	6.80		
Roc de Marsal	a	2[a]	L	7.80	7.00		
Roc de Marsal	b	no wear	R	7.77	6.72		
Subaluk	2	not specified	L	6.5	5.2	6.2	5.4
Subaluk	2	not specified	R	5.9	5.6		
Engis	2	3[a]	L	7.50	6.64		
La Quina	33	4[a]	R	7.59	6.96		
Kebara	22	4[a]	L	7.67	7.34		
Portel-Ouest Cave	LP_20	6[a]	R	7.00	6.80		
Portel-Ouest Cave	LP_23	6[a]	L	6.90	7.20		
Beau de l'Aubesier6	Aubesier 6	3[a]	L	8.60	7.10		
Grotte du Bison (Arcy sur Cure)	O11-192	not specified	L	7.70	7.00		
Grotte du Renne (Arcy-sur-Cure)	37	1[b]	L	8.00	7.50		
Grotte du Renne (Arcy-sur-Cure)	38	0[b]	L	7.40	7.00		
Qafzeh	15	4[a]	R	7.92	6.86		
Qafzeh	12	4[a]	R	8.63	7.47		
Fourneau du Diable	900	not specified	R	7.6	6.8		
Pavlov13	900	5[a]	R	6.8	6.4		
Pavlov14	903	5[a]	R	6.1	5.8		
Pavlov	908	not specified	L	5.8	6.1		
Pavlov	909	not specified	L	6.2	6.5		
La Madeleine	IV	not specified	R	7.2	6.5		
St. Germain La Riviere	8	not specified	R	7.1	6.3		
Aveline's Hole	M1.11.242	not specified	L	5.9	5.5		
Rochereil	3	not specified	R	6.1	6.26		
El Cingle Vermell	K8.T7	not specified	L	6.4	5.7		
Ofnet	1,037,201,389	not specified	R	7.37	6.23		
Ofnet	1,038,048,611	not specified	L	7.62	6.98		
Ofnet	1,041,861,111	not specified	L	7.1	6.01		
Ofnet	1,042,708,333	not specified	R	7.18	6.16		
Ofnet	1,043,979,167	not specified	R	7.1	5.99		
Felsstalle Muhlen	900	not specified	L	5.8	5.2		

Arene Candide (Epi-Grav.)	11	not specified	L	7.3	6.6		
Arene Candide (Epi-Grav.)	8	not specified	L	7.8	7.2		
Hoedic	7b	not specified	L	6.03	5.52		
Muge Arruda	1.1937.P	not specified	R	7.4	6.8		
Muge Arruda	176c.L	not specified	L	6.82	6.49		
Muge Arruda	901.P	not specified	L	7.32	6.03		
Muge Arruda	916.L	not specified	L	7.28	6.17		
Skateholm2	XIII	not specified	L	7.36	7		
Vlasac (Ia + Ib)	53	not specified	L	7	5.7		
Obristvi	0.118055556	not specified	R	7	6.6		
Obristvi	0.201388889	not specified	R	7	6.7		
Krskany	0.586111111	not specified	L	7.2	6.6		
Krskany	28.65	not specified	L	6.9	5.3		
Krskany	30.65	not specified	L	6.9	6.5		
Krskany	38.65	not specified	L	6.6	6.6		
Krskany	50.65	not specified	R	7.5	7		
Krskany	60.65	not specified	L	7.3	6.5		
Krskany	67.65	not specified	R	7	6.5		
Krskany	68.65	not specified	L	6.5	6		
Vedrovice	0.802083333	not specified	R	6.7	5.9		
Vedrovice	0.170833333	not specified	L	6.9	6.6		
Vedrovice	0.214583333	not specified	L	6.9	6.4		
Vedrovice	84.80	not specified	R	6.7	5.8		
Szegvar-Tzkoves	71.27.23.62	not specified	R	6.7	6		
Szany	10181	not specified	R	6.6	5.9		
Zalavar-Var	8802	not specified	L	8.3	6.2		
Keszthely	13.80.2.8	not specified	L	7.1	6		
Tiszfüred -Mojores	68.133.32.0D49	not specified	L	6.6	5.5		
BP Wekerle-Telep	9563	not specified	L	6.9	6		
Budapest-Timur ut	1988.IV.12 16.2	not specified	R	6.5	5.5		
Tiszalök	82.1.101	not specified	L	6.6	5.8		
Pilismar—t	9386	not specified	L	6.3	5.5		
Grotte des Enfants	1	not specified	L	7	6.4		
Grotte des Enfants	2	not specified	L	7.26	6.62	7.26	6.73
Grotte des Enfants	2	not specified	R	7.26	6.84		
La Geniere	1	not specified	L	7.08	6.75	7.08	6.67
La Geniere	1	not specified	R	7.07	6.58		
Hohlenstein	3	not specified	L	6.92	5.87	6.93	5.92
Hohlenstein	3	not specified	R	6.94	5.96		
Ofnet	1,030,840,278	not specified	L	7.31	6.17	7.24	6.31
Ofnet	1,030,840,278	not specified	R	7.16	6.44		
Ofnet	1,032,958,333	not specified	L	7.07	6.49	7.11	6.53
Ofnet	1,032,958,333	not specified	R	7.14	6.56		

Ofnet	1,033,381,944	not specified	L	7.51	6.05	7.4	6.04
Ofnet	1,033,381,944	not specified	R	7.28	6.02		
Ofnet	2484.11A	not specified	L	7.49	6.66	7.5	6.68
Ofnet	2484.11A	not specified	R	7.5	6.7		
Ofnet	103.55	not specified	L	7.74	7.03	7.71	7.05
Ofnet	103.55	not specified	R	7.68	7.06		
Ofnet	1,038,472,222	not specified	L	7.22	7.08	7.22	7.03
Ofnet	1,038,472,222	not specified	R	7.22	6.98		
Ofnet	1,039,319,444	not specified	L	7.73	6.43	7.73	6.47
Ofnet	1,039,319,444	not specified	R	7.72	6.51		
Ofnet	1,039,743,056	not specified	L	7.35	6.99	7.42	6.92
Ofnet	1,039,743,056	not specified	R	7.48	6.84		
Schnellnecker Wand	2	not specified	L	6	6.1	6.05	6.1
Schnellnecker Wand	2	not specified	R	6.1	6.1		
Arene Candide (Epi-Grav.)	6	not specified	L	6.9	6.3	6.95	6.2
Arene Candide (Epi-Grav.)	6	not specified	R	7	6.1		
Muge Arruda	4.P	not specified	L	7.28	6.19	7.25	6.26
Muge Arruda	4.P	not specified	R	7.21	6.32		
Muge Arruda	48.L	not specified	L	7.02	6.32	6.95	6.26
Muge Arruda	48.L	not specified	R	6.88	6.19		
Muge Arruda	917.L	not specified	L	7.58	6.97	7.49	6.85
Muge Arruda	917.L	not specified	R	7.39	6.72		
Obristvi	0.079861111	not specified	L	7.2	7.2	7.15	7.2
Obristvi	0.079861111	not specified	R	7.1	7.2		
Obristvi	0.159722222	not specified	L	7.2	7	7.35	6.95
Obristvi	0.159722222	not specified	R	7.5	6.9		
Krskany	13a.64	not specified	L	7.2	5.9	7.2	5.95
Krskany	13a.64	not specified	R	7.2	6		
Krskany	40.65	not specified	L	6.6	6.9	6.75	6.85
Krskany	40.65	not specified	R	6.9	6.8		
Krskany	49.65	not specified	L	7.1	5.8	7.1	5.8
Krskany	49.65	not specified	R	7.1	5.8		
Krskany	54.65	not specified	L	6.7	6	6.7	6.05
Krskany	54.65	not specified	R	6.7	6.1		
Krskany	71.65	not specified	L	6.1	5.7	6.15	5.7
Krskany	71.65	not specified	R	6.2	5.7		
Krskany	74.65	not specified	L	6.7	6.1	6.7	6.15
Krskany	74.65	not specified	R	6.7	6.2		
Vedrovice	109.84	not specified	L	6.9	6.5	7	6.55
Vedrovice	109.84	not specified	R	7.1	6.6		
Vedrovice	0.71875	not specified	L	6.9	6.2	6.9	6.2
Vedrovice	0.71875	not specified	R	6.9	6.2		

Vedrovice	0.885416667	not specified	L	7.3	6	7.25	5.95
Vedrovice	0.885416667	not specified	R	7.2	5.9		
Vedrovice	28.76	not specified	L	6.8	6.3	6.8	6.3
Vedrovice	28.76	not specified	R	6.8	6.3		
Vedrovice	39.76	not specified	L	6.3	5.8	6.5	5.7
Vedrovice	39.76	not specified	R	6.7	5.6		
Vedrovice	40.76	not specified	L	6.9	6.5	7.1	6.6
Vedrovice	40.76	not specified	R	7.3	6.7		
Vedrovice	0.269444444	not specified	L	6.2	5.6	6.2	5.65
Vedrovice	0.269444444	not specified	R	6.2	5.7		
Vedrovice	78.79	not specified	L	7.1	6.5	6.85	6.5
Vedrovice	78.79	not specified	R	6.6	6.5		
Szegvar-Tzkoves	71.27.11.47	not specified	L	7.1	5.9	7.05	5.7
Szegvar-Tzkoves	71.27.11.47	not specified	R	7	5.5		
Keszthely	13.80.3.12	not specified	L	6.6	6.3	6.75	6.3
Keszthely	13.80.3.12	not specified	R	6.9	6.3		
BP Wekerle-Telep	9551	not specified	L	6.8	6.2	6.8	6.15
BP Wekerle-Telep	9551	not specified	R	6.8	6.1		
Tiszfüred	79.5.102.111	not specified	L	7.3	6.1	7.45	6.15
Tiszfüred	79.5.102.111	not specified	R	7.6	6.2		
Tiszfüred -Honfoglalaskor	79.5.108.117	not specified	L	6.3	5.7	6.35	5.65
Tiszfüred -Honfoglalaskor	79.5.108.117	not specified	R	6.4	5.6		
Tiszfüred -Honfoglalaskor	79.5.16.17	not specified	L	7.3	5.9	7.4	5.85
Tiszfüred -Honfoglalaskor	79.5.16.17	not specified	R	7.5	5.8		
Csontuaz	2.79.8.23	not specified	L	6.9	5.8	7	5.8
Csontuaz	2.79.8.23	not specified	R	7.1	5.8		
Tiszalök	82.1.176	not specified	L	7.2	6.2		
Tiszalök	82.1.176	not specified	R	7.1	6.2	7.15	6.2
Tiszalök	3,417,453,704	not specified	L	6.5	5.9	6.4	5.8
Tiszalök	3,417,453,704	not specified	R	6.3	5.7		
Nyarsapat	9327	not specified	L	7	5.2	7	5.15
Nyarsapat	9327	not specified	R	7	5.1		
Nyarsapat	9345	not specified	L	7.4	5.9	7.4	6
Nyarsapat	9345	not specified	R	7.4	6.1		
Abri Pataud	P6 (AP/58-2-F2283)	3[c]	R	7.60	6.90		
T64	T64	3[a]	L	6.92	6.37		
T43	T43	3[a]	R	6.68	5.97		
T16	T16	2[a]	L	7.16	5.79		
3b	3b	4[a]	R	7.54	5.85		
3a	3a	3[a]	L	7.42	5.84		
2b	2b	4[a]	R	7.06	6.37		
1b	1b	4[a]	R	6.47	5.52		

1	1	4ª	R	6.38	5.56
T54	T54	4ª	R	7.13	6.67
T53	T53	3ª	R	6.73	6.39
4	4	3ª	R	7.12	6.22
T124	T124	4ª	R	7.26	5.55
T76	T76	4ª	R	6.72	6.19
T75	T75	3ª	R	7.31	6.30
T72	T72	3ª	R	6.72	6.37
T71	T71	3ª	R	5.49	5.78
T70	T70	3ª	R	6.98	5.50
T63	T63	2ª	R	6.95	6.31
T61	T61	3ª	R	7.34	6.56
T48	T48	2ª	L	7.46	6.80

Abbreviations: MD = mesiodistal diameter; BL = buccolingual diameter; R = right; L = left; Ind# = ID code.

SOM Table S4
Dental cervical dimensions and pulp chamber index.

	Cervical		Pulp index
ID	MD	BL	
Riparo Broion1	6.23	6.22	4.0
Roc de Marsal	6.28	6.38	7.93
Engis2	5.76	5.78	2.16
KRPD23	6.50	6.61	11.01
LQ33	5.69	6.14	16.71
KebaraKMH22	5.99	6.45	6.76
Qafzeh12	5.80	6.06	11.63
Qafzeh15	6.40	5.73	8.55
Pav13	5.46	5.45	18.36
Pav14	5.30	5.05	22.92
T16	5.56	5.09	19.02
T48	NA	NA	15.22
3a	5.39	5.19	NA
3b	5.42	5.02	6.54
2b	5.69	5.68	27.21
1b	5.02	4.94	10.56
1	4.81	4.96	12.78
T54	5.10	5.64	14.40
T53	5.45	5.91	8.62
4	5.91	5.61	10.21
T124	5.31	4.90	10.47
T76	5.18	5.54	10.63
T75	6.24	5.60	11.15
T72	5.07	5.73	11.61
T71	4.41	5.46	6.38
T70	4.81	5.06	16.43
T63	5.26	5.60	14.80
T61	5.30	5.78	10.86
T64	5.48	5.63	9.47
T43	4.79	5.00	NA

Abbreviations: MD = mesiodistal diameter; BL= buccolingual diameter; pulp index = coronal pulp chamber index.

SOM Table S5

Significant differences in the distribution of enamel thickness between NEA and RHS at 25%, 50%, and 75% of the distance between the cervical plane and the 100 µm bin closest to the bicervical diameter.

Percentile	Test statistic (W)	*p*
0.25	11	0.011
0.5	17	0.04
0.75	16	0.034

Abbreviations: NEA = Neanderthal; RHS = recent *Homo sapiens*.

SOM Table S6

3D values of enamel thickness for each individual.

	Sample	Wear[a]	EV	DV	EDJ	3D AET	3D RET	LEV	LDV	LEDJ	3D LAET	3D LRET
	RB1	4		100.1	83.88				44.04	31.53	NA	NA
NEA												
	Roc de	2	47.9	80.17	73.51	0.65	15.1	23.7	65.07	47.95	0.49	12.30
	Engis2	3	38.0	107.3	83.86	0.45	9.54	5.36	33.26	25.50	0.21	6.54
	KRPD23	3	50.9	132.4	114.6	0.44	8.72	39.2	110.5	94.11	0.40	8.25
	KebaraKMH2	4	35.4	123.9	103.6	0.34	6.85	15.3	92.47	63.95	0.24	5.30
	LQ33	4	29.7	86.95	79.32	0.37	8.45	11.3	46.61	44.94	0.25	6.99
EHS												
	Qafzeh12	4	71.5	130.9	120.1	0.60	11.7	47.4	104.2	91.34	0.52	11.04
	Qafzeh15	4	50.9	89.16	85.51	0.60	13.3	16.9	44.21	29.05	0.58	16.53
UPH												
	Pavlov13	5	24.7	65.76	53.29	0.46	11.5	11.5	55.56	51.55	0.22	5.86
	Pavlov14	5	14.8	60.82	50.07	0.30	7.53	12.8	46.30	42.44	0.30	8.43
RHS												
	T16	2	35.1	79.28	82.56	0.43	9.92	23.3	66.61	65.08	0.36	8.87
	T48	2	52.4	93.91	90.49	0.58	12.7	35.6	75.84	72.77	0.49	11.57
	T63	2	38.3	78.93	81.94	0.47	10.9	29.0	66.23	71.90	0.40	9.98
	T64	3	41.1	76.86	80.58	0.51	12.0	26.6	64.60	62.90	0.42	10.56
	T53	3	34.9	89.69	81.90	0.43	9.54	22.8	77.30	69.17	0.33	7.74
	4	3	44.7	79.12	81.53	0.55	12.7	22.9	61.73	56.94	0.40	10.21
	T75	3	38.4	84.36	82.81	0.46	10.5	20.0	67.72	58.60	0.46	8.40
	T72	3	36.2	84.75	78.10	0.46	10.5	21.7	69.27	59.22	0.43	8.93
	T71	3	26.0	62.83	64.48	0.40	10.1	11.1	47.36	39.11	0.34	7.87
	T70	3	32.9	67.25	75.77	0.44	10.7	23.4	53.80	61.85	0.37	10.06
	T61	3	41.9	79.67	81.21	0.52	12.0	23.7	62.14	56.54	0.42	10.59
	3a	3	79.4	83.80	83.20	0.95	21.8	30.5	78.86	74.18	0.41	9.61
	T43	3	35.6	67.92	73.09	0.49	11.9	17.1	54.84	47.10	0.36	9.60
	1	4	24.1	61.46	66.01	0.37	9.29	8.77	37.25	36.16	0.24	7.26
	1b	4	23.0	62.88	65.18	0.35	8.90	7.47	33.52	30.94	0.24	7.49
	2b	4	28.4	81.33	73.11	0.39	8.98	13.6	49.03	47.18	0.29	7.91
	3b	4	43.9	85.95	83.24	0.53	11.9	15.1	54.93	42.27	0.36	9.43
	T54	4	44.8	94.11	85.02	0.53	11.5	28.8	73.17	63.34	0.46	10.90
	T124	4	45.3	69.10	77.31	0.59	14.2	26.6	54.64	57.79	0.46	12.17
	T76	4	34.2	73.17	77.07	0.44	10.6	20.3	59.45	47.35	0.43	11.00

Abbreviations: NEA = Neanderthals; EHS = early *Homo sapiens*; UPHS = Upper Paleolithic *H. sapiens*; RHS = recent *H. sapiens*; EV = enamel volume; DV = dentine volume; EDJ = enamel-dentine junction; AET = average enamel thickness; RET = relative enamel thickness; LEV = lateral

enamel thickness; LDV = lateral dentine volume; LEDJ = lateral enamel-dentine junction; LAET = lateral average enamel thickness; LRET = lateral relative enamel thickness.

[a] Molnar (1971).

SOM Table S7
Overview of DNA extracts and libraries.

Sample	Amount of powder used	Library preparation setup	Library ID	Number of DNA molecules	Number of spiked-in control oligo
Tooth from Riparo Broion	~5 mg	1	A19718	3.11E+09	7.38E+05
		2	A23035	3.31E+09	7.12E+05
			A23036	3.51E+09	1.14E+06
Extraction negative control	—	1	A19724	8.94E+07	9.59E+05
	—	2	A22982	7.74E+07	1.33E+06
Library preparation negative control	—	1	A19715	5.34E+07	7.69E+05
	—	2	A23038	9.87E+07	9.25E+05

SOM Table S8

Sequencing summary statistics of the libraries prepared from the tooth powder.

Library ID	Raw number of sequences	Number of sequences (L ≥ 35 bp)	Reference used for mapping	Mapped sequences (L ≥ 35 bp, MQ ≥ 25)	% mapped (L ≥ 35 bp, MQ ≥ 25)	Unique sequences	Deaminated (first or last 3 positions)[a]
A19718	439,249	219,230	rCRS	147,372	67.2	19,516	7380
			Spy 94a	148,621	67.8	19,789	7516
A23035	672,882	364,560	rCRS	243,572	66.8	16,902	6373
			Spy 94a	246,528	67.6	17,145	6507
A23036	663,637	357,712	rCRS	247,531	69.2	18,122	6994
			Spy 94a	249,473	69.7	18,329	7106
Total	1,775,768	941,502	rCRS	638,475	67.8	54,540	20,747
			Spy 94a	644,622	68.5	55,263	21,129

Abbreviations: rCRS = revised Cambridge Reference Sequence (Andrews et al., 1999); L= length; MQ = mapping quality; bp = base pairs.

[a] 'Deaminated' refers to sequences carrying a C to T substitution to the reference genome used for mapping within their first three or last three positions.

SOM Table S9

Sequencing summary statistics of the negative controls.

Library ID	Raw number of sequences	Number of sequences (L ≥35bp)	Reference used for mapping	Mapped sequences (L ≥ 35 bp, MQ ≥ 25)	% mapped (L ≥ 35 bp, MQ ≥ 25)	Unique sequences	Deaminated (first or last 3 positions) [a]
A19724 (ENC)	78,098	33,072	rCRS	29,404	88.9	1996	30
			Spy 94a	28,613	86.5	1940	42
A22982 (ENC)	92,648	34,382	rCRS	30,442	88.5	40	4
			Spy 94a	30,438	88.5	39	1
A19715 (LNC)	78,540	33,391	rCRS	21,919	65.6	62	1
			Spy 94a	20,335	60.9	58	2
A23038 (LNC)	81,451	26,473	rCRS	24,711	93.3	16	1
			Spy 94a	24,706	93.3	15	1

Abbreviations: ENC = extraction negative control; LNC = library preparation negative control; L = length; MQ = mapping quality; bp = base pairs.

[a] 'Deaminated' refers to sequences carrying a C to T substitution to the reference genome used for mapping within their first three or last three positions.

SOM Table S10

Present-day human contamination estimates based on the alleles seen at diagnostic positions where the mitochondrial genomes of present-day humans and Neandertals differ. Numbers in brackets correspond to sequences from deaminated DNA fragments, i.e., with at least one C-to-T substitution within the first three or last three positions. Sequences are considered conflicting if they overlap multiple informative positions and carry both Neandertal and present-day human alleles.

Library ID	Reference used for mapping	Neandertal state	Present-day human state	Conflicting	Contamination estimate (%)	Binomial 95% Confidence Intervals
A19718	rCRS	718 [261]	100 [2]	0	12.2 [0.8]	10.1–14.7 [0.1–2.7]
	Spy 94a	753 [292]	97 [3]	0	11.4 [1.0]	9.4–13.7 [0.2–2.9]
A23035	rCRS	511 [204]	126 [7]	1 [0]	19.8 [3.3]	16.8–23.1 [1.3–6.7]
	Spy 94a	541 [226]	123 [8]	1 [0]	18.5 [3.4]	15.6–21.7 [1.5–6.6]
A23036	rCRS	555 [219]	117 [7]	0	17.4 [3.1]	14.6–20.5 [4.3–11.3]
	Spy 94a	582 [237]	111 [8]	0	16.0 [3.3]	13.4–19.0 [1.4–6.3]
Total	rCRS	1,784 [684]	343 [16]	1 [0]	16.1 [2.3]	14.6–17.8 [1.3–3.7]
	Spy 94a	1,876 [755]	331 [19]	1 [0]	15.0 [2.5]	13.5–16.6 [1.5–3.8]

SOM Table S11

Best substitution models (in bold type) according to the three model selection measures computed by jModelTest 2.1.10. These measures are the Bayesian information criterion (BIC), a measure based on decision theory (DT) and the corrected Akaike information criterion (AICc).

Measure	Model	Rank	Log-likelihood	Measure value
AICc	**GTR+I+G**	**1**	**-34,349.53685**	**69,096.133587**
AICc	TrN+I+G	2	-34,353.54238	69,097.990361
AICc	GTR+I	3	-34,365.65403	69,126.316250
BIC	**TrN+I+G**	**1**	**-34,353.54238**	**70,568.752461**
BIC	GTR+I+G	2	-34,349.53685	70,589.679241
BIC	TrN+I	3	-34,369.29753	70,590.616814
DT	**TrN+I+G**	**1**	**-34,353.54238**	**0.000000**
DT	GTR+I	2	-34,365.65403	0.004229
DT	GTR+I+G	3	-34,349.53685	0.004806

SOM Table S12

Marginal likelihoods of the different tested clock and tree models obtained from a path sampling approach. The two equally good best models are marked in bold.

Clock model	Tree model	Marginal log-likelihood
Strict	Coalescent with constant population size	-34910.74992730804
Relaxed (uncorrelated lognormal)	Coalescent with constant population size	-34909.75702973354
Strict	**Bayesian Skyline**	**-34888.544717899014**
Relaxed (uncorrelated lognormal)	**Bayesian Skyline**	**-34887.52148846142**

SOM Table S13

Estimates of molecular age and divergence times (years before present). Estimates were obtained from three Markov chain Monte Carlo runs of 75,000,000 iterations each (sampling parameter values and trees every 5000 iterations, with a burn-in of 15,000,000 iterations). Values involving Riparo Broion 1 are marked in bold.

Parameter	Mean	95% HPD lower	95% HPD upper	ESS
Human-chimpanzee TMRCA	5,989,400	5,163,400	6,873,200	2564
Archaic and modern human TMRCA	869,900	784,170	955,120	1656
Neandertal and modern human TMRCA	436,130	383,690	491,430	3805
Modern human TMRCA	151,520	128,540	175,680	9517
Neandertal TMRCA	281,920	235,650	330,610	2577
Riparo Broion – Goyet - Spy cluster TMRCA	**47,037**	**43,237**	**51,387**	**5838**
Riparo Broion age	**38,932**	**30,118**	**46,408**	**18,972**
Scladina I-4A age	121,330	81,355	162,710	1824
Hohlenstein-Stadel Neandertal age	132,660	73,694	195,840	3743
Altai Neandertal (Denisova 5) age	132,760	93,521	173,070	1624
Vindija 33.17 age	50,285	41,415	59,663	6862
Vindija 33.19 age	44,606	35,467	52,635	9327
Vindija 33.25 age	44,919	34,256	56,400	5514
Mezmaiskaya 1 age	100,700	61,636	137,130	2549
Okladnikov 2 age	92,375	66,808	117,140	1488
Goyet Q305-7 age	40,349	32,262	46,380	15,674
Goyet Q374a-1 age	40,345	32,635	46,469	16,715
Goyet Q57-1 age	44,876	33,829	56,336	5443
Denisova 11 age	99,460	76,415	122,470	1218
Denisova 3 age	84,248	59,714	100,000	656
Denisova 4 age	89,047	58,399	113,760	646
Denisova 8 age	184,810	113,870	261,910	1093
Denisova 2 age	218,670	150,540	290,280	987
Sima de los Huesos	388,270	263,520	501,160	1368

Abbreviations: TMRCA = time to the most recent common ancestor; HPD = highest posterior density; ESS = effective sample size.

SOM Table S14

List of the main European Late Mousterian sites (<50 ka) where Neanderthal remains have been found, with details of the context and potential attribution to funerary practice.

Site	Geography	Collapsed cave mouth <10m	Cave mouth ≤10m	Shelter	Inner cave >15m	Burial	Cannibalism
La Ferrassie	France		X			X	
Le Moustier	France		X			?	
Saint-Cesair	France		X			X	
Arcy-sur-Cure	France				X		
Portel-Ouest	France				X		
El Sidrón	Spain				X		X
Sima de las Palomas	Spain				X		
Zafarraya	Spain				X		X
El Salt	Spain			X			
Devil's Tower Shelter	Gibraltar				X		
Vindija	Croatia				X		
Spy	Belgium				X		X
Goyet	Belgium				X		
Kulna_1	Czech Republic				X		
Lakonis	Greece	X					
Fumane	Italy		X				
Riparo Broion	Italy			X			
Cavallo	Italy		X				
Tagliente	Italy			X			

SOM Table S15

Raw data for analysis using code in SOM S8.

	taxon	MD	BL	side
Valdegoba_2	NEA	6.6	5.8	L
Dederiyeh_1	NEA	7.8	7.3	R
Krapina_D23	NEA	8.38	7.3	L
Krapina_7	NEA	8.2	6.8	MEAN
Pinar_7	NEA	7.9	6.8	L
RocdeMarsal_a	NEA	7.8	7	L
RocdeMarsal_b	NEA	7.77	6.72	R
Subaluk_2	NEA	6.2	5.4	MEAN
Engis_2	NEA	7.5	6.64	L
LaQuina_33	NEA	7.59	6.96	R
Kebara_22	NEA	7.67	7.34	L
Portel-OuestCave_LP_20	NEA	7	6.8	R
Portel-OuestCave_LP_23	NEA	6.9	7.2	L
BeaudelAubesier6_Aubesier6	NEA	8.6	7.1	L
GrotteduBison(ArcysurCure)_O11-192	NEA	7.7	7	L
GrotteduRenne(Arcy-sur-Cure)_37	NEA	8	7.5	L
GrotteduRenne(Arcy-sur-Cure)_38	NEA	7.4	7	L
Qafzeh_15	EHS	7.92	6.86	R
Qafzeh_12	EHS	8.63	7.47	R
FourneauduDiable_900	UPMHS	7.6	6.8	R
Pavlov13_900	UPMHS	6.8	6.4	R
Pavlov14_903	UPMHS	6.1	5.8	R
Pavlov_908	UPMHS	5.8	6.1	L
Pavlov_909	UPMHS	6.2	6.5	L
LaMadeleine_IV	UPMHS	7.2	6.5	R
St.GermainLaRivière_8	UPMHS	7.1	6.3	R
AvelinesHole_M1.11.242	UPMHS	5.9	5.5	L
Rochereil_3	UPMHS	6.1	6.26	R
ElCingleVermell_K8.T7	UPMHS	6.4	5.7	L
Ofnet_103.720138888889	UPMHS	7.37	6.23	R
Ofnet_103.804861111111	UPMHS	7.62	6.98	L
Ofnet_104.186111111111	UPMHS	7.1	6.01	L
Ofnet_104.270833333333	UPMHS	7.18	6.16	R
Ofnet_104.397916666667	UPMHS	7.1	5.99	R
FelsstalleMuhlen_900	UPMHS	5.8	5.2	L
AreneCandide(Epi-Grav.)_11	UPMHS	7.3	6.6	L
AreneCandide(Epi-Grav.)_8	UPMHS	7.8	7.2	L
Hoedic_7b	UPMHS	6.03	5.52	L
MugeArruda_1.1937.P	UPMHS	7.4	6.8	R

MugeArruda_176c.L	UPMHS	6.82		6.49		L
MugeArruda_901.P	UPMHS	7.32		6.03		L
MugeArruda_916.L	UPMHS	7.28		6.17		L
Skateholm2_XIII	UPMHS	7.36			7	L
Vlasac(Ia+Ib)_53	UPMHS		7	5.7		L
Obristvi _0.118055555555556	UPMHS		7	6.6		R
Obristvi _0.201388888888889	UPMHS		7	6.7		R
Krskany_0.586111111111111	UPMHS	7.2		6.6		L
Krskany_28.65	UPMHS	6.9		5.3		L
Krskany_30.65	UPMHS	6.9		6.5		L
Krskany_38.65	UPMHS	6.6		6.6		L
Krskany_50.65	UPMHS	7.5			7	R
Krskany_60.65	UPMHS	7.3		6.5		L
Krskany_67.65	UPMHS		7	6.5		R
Krskany_68.65	UPMHS	6.5			6	L
Vedrovice_0.802083333333333	UPMHS	6.7		5.9		R
Vedrovice_0.170833333333333	UPMHS	6.9		6.6		L
Vedrovice_0.214583333333333	UPMHS	6.9		6.4		L
Vedrovice_84.80	UPMHS	6.7		5.8		R
Szegvar-Tzkoves_71.27.23.62	UPMHS	6.7			6	R
Szany_10181	UPMHS	6.6		5.9		R
Zalavar-Var_8802	UPMHS	8.3		6.2		L
Keszthely_13.80.2.8	UPMHS	7.1			6	L
Tiszafüred-Mojores_68.133.32.0D49	UPMHS	6.6		5.5		L
BPWekerle-Telep_9563	UPMHS	6.9			6	L
Budapest-Timurut_1988.IV.1216.2	UPMHS	6.5		5.5		R
Tiszalök_82.1.101	UPMHS	6.6		5.8		L
Pilismar—t_9386	UPMHS	6.3		5.5		L
GrottedesEnfants_1	UPMHS		7	6.4		L
GrottedesEnfants_2	UPMHS	7.26		6.73		MEAN
LaGeniere_1	UPMHS	7.075		6.665		MEAN
Hohlenstein_3	UPMHS	6.93		5.915		MEAN
Ofnet_103.084027777778	UPMHS	7.235		6.305		MEAN
Ofnet_103.295833333333	UPMHS	7.105		6.525		MEAN
Ofnet_103.338194444444	UPMHS	7.395		6.035		MEAN
Ofnet_2484.11A	UPMHS	7.495		6.68		MEAN
Ofnet_103.55	UPMHS	7.71		7.045		MEAN
Ofnet_103.847222222222	UPMHS	7.22		7.03		MEAN
Ofnet_103.931944444444	UPMHS	7.725		6.47		MEAN
Ofnet_103.974305555556	UPMHS	7.415		6.915		MEAN
SchnellneckerWand_2	UPMHS	6.05		6.1		MEAN
AreneCandide(Epi-Grav.)_6	UPMHS	6.95		6.2		MEAN
MugeArruda_4.P	UPMHS	7.245		6.255		MEAN

MugeArruda_48.L		UPMHS	6.95		6.255		MEAN
MugeArruda_917.L		UPMHS	7.485		6.845		MEAN
Obristvi _0.0798611111111111		UPMHS	7.15		7.2		MEAN
Obristvi _0.159722222222222		UPMHS	7.35		6.95		MEAN
Krskany_13a.64		UPMHS	7.2		5.95		MEAN
Krskany_40.65		UPMHS	6.75		6.85		MEAN
Krskany_49.65		UPMHS	7.1		5.8		MEAN
Krskany_54.65		UPMHS	6.7		6.05		MEAN
Krskany_71.65		UPMHS	6.15		5.7		MEAN
Krskany_74.65		UPMHS	6.7		6.15		MEAN
Vedrovice_109.84		UPMHS		7	6.55		MEAN
Vedrovice_0.71875		UPMHS	6.9		6.2		MEAN
Vedrovice_0.885416666666667		UPMHS	7.25		5.95		MEAN
Vedrovice_28.76		UPMHS	6.8		6.3		MEAN
Vedrovice_39.76		UPMHS	6.5		5.7		MEAN
Vedrovice_40.76		UPMHS	7.1		6.6		MEAN
Vedrovice_0.269444444444444		UPMHS	6.2		5.65		MEAN
Vedrovice_78.79		UPMHS	6.85		6.5		MEAN
Szegvar-Tzkoves_71.27.11.47		UPMHS	7.05		5.7		MEAN
Keszthely_13.80.3.12		UPMHS	6.75		6.3		MEAN
BPWekerle-Telep_9551		UPMHS	6.8		6.15		MEAN
Tiszfüred_79.5.102.111		UPMHS	7.45		6.15		MEAN
Tiszafüred-Honfoglalaskor_79.5.108.117		UPMHS	6.35		5.65		MEAN
Tiszafüred-Honfoglalaskor_79.5.16.17		UPMHS	7.4		5.85		MEAN
Csontuaz_2.79.8.23		UPMHS		7	5.8		MEAN
Tiszalök_82.1.176		UPMHS	7.15		6.2		MEAN
Tiszalök_3.4174537037037		UPMHS	6.4		5.8		MEAN
Nyarsapat_9327		UPMHS		7	5.15		MEAN
Nyarsapat_9345		UPMHS	7.4			6	MEAN
AbriPataud_P6(AP/58-2-F2283)		UPMHS	7.6		6.9		R
T64		RHS	6.92		6.37		L
T43		RHS	6.68		5.97		R
T16		RHS	7.16		5.79		L
3b		RHS	7.54		5.85		R
3a		RHS	7.42		5.84		L
2b		RHS	7.06		6.37		R
1b		RHS	6.47		5.52		R
	1	RHS	6.38		5.56		R
T54		RHS	7.13		6.67		R
T53		RHS	6.73		6.39		R
	4	RHS	7.12		6.22		R
T124		RHS	7.26		5.55		R
T76		RHS	6.72		6.19		R

T75	RHS	7.31	6.3	R
T72	RHS	6.72	6.37	R
T71	RHS	5.49	5.78	R
T70	RHS	6.98	5.5	R
T63	RHS	6.95	6.31	R
T61	RHS	7.34	6.56	R
T48	RHS	7.46	6.8	L

SOM Table S16

Raw data for analysis using code in SOM S13.

	Wear Stage	taxon	Index	AET	RET	Lat-AET	Lat_ RET
ROC_DE_MARSAL	2	NEA	7.9299216229	0.6517480615	15.1150337153	0.4946819604	12.2988868008
Engis_2	3	NEA	2.1647624775	0.4533746721	9.539447851	0.2101960784	6.536077518
Kebara KMH22	3	NEA	6.7589488483	0.3417574998	6.8542119731	0.2398749023	5.3045822971
KRP_D23	4	NEA	11.0125780472	0.4442312723	8.7150403879	0.3959196685	8.2503660475
LQ_33	5	NEA	16.7131516842	0.3744326778	8.4518260156	0.2514463729	6.9869184523
Dente 1	2	RHS	12.7785234899	0.3664596273	9.2859986666	0.2425331858	7.2621031375
Dente 1b	2	RHS	10.5608591885	0.3539429273	8.9008003713	0.2414350356	7.487996323
Dente 2b	2	RHS	27.2078319396	0.3890028724	8.9784744418	0.2895294616	7.9105278716
Dente 3b	3	RHS	6.5355907519	0.5278712158	11.961326744	0.35841022	9.4285270636
Dente T16	3	RHS	19.0211679928	0.4259932171	9.9162652885	0.3594038107	8.8661729694
Dente T48	3	RHS	15.2162447257	0.5792905293	12.744588425	0.4898996839	11.5737576587
Dente T64	3	RHS	9.4736842105	0.5101762224	11.9992311722	0.4238473768	10.5632768028
DenteT54	3	RHS	14.4048107148	0.5271700776	11.5896990941	0.4557941269	10.8974371556
DenteT53	3	RHS	8.6157826649	0.426984127	9.5388727633	0.3296226688	7.7379141437
Dente4	3	RHS	10.2057346509	0.5487550595	12.7825189305	0.4035827187	10.2117569407
Dente T124	3	RHS	10.4685212299	0.5862113569	14.2854813584	0.4616715695	12.1664226832
Dente T76	4	RHS	10.6307821699	0.4442714415	10.6219449269	0.4291446674	10.9956211326
Dente T75	4	RHS	11.1488481985	0.4643159039	10.5868811051	0.3424914676	8.4025435741
Dente T72	4	RHS	11.6067561715	0.4645326504	10.5755511203	0.3665991219	8.9264002834
Dente T71	4	RHS	6.3766891892	0.4044665012	10.1740422864	0.2848376374	7.8727563396
Dente T70	4	RHS	16.4312267658	0.4351326382	10.7001754048	0.3796281326	10.0561319533
Dente T63	4	RHS	14.7969198249	0.4677813034	10.9050792328	0.4037552156	9.979295751
Dente T61	4	RHS	10.8625683939	0.5166851373	12.0077332063	0.4193491334	10.5873027832
Dente T43	3	RHS	6.8745441284	0.4880284581	11.9613240175	0.364543524	9.59511622
Dente 3a	4	RHS	8.977935582	0.9548076923	21.8189863026	0.412240496	9.61313544

SOM Table S17

Raw data for analysis using code in SOM S5.

	taxon	Outline.symmetry	Buccal.bulging	Mesial.crest
R_d_Marsal	NEA	1	1	0
Engis_2	NEA	1	1	1
LQ_33	NEA	1	1	1
KRP_D23	NEA	1	1	1
KMH_22	NEA	1	1	1
Qafzeh_12	EHS	0	1	1
Qafzeh_15	EHS	0	0	0
1	RHS	0	1	0
1b	RHS	0	1	0
2b	RHS	1	0	1
3a	RHS	1	1	0
3b	RHS	1	1	1
T16	RHS	0	0	0
T43	RHS	0	0	0
T48	RHS	0	1	1
T64	RHS	0	0	1
T54	RHS	1	1	1
T53	RHS	1	1	1
4	RHS	0	0	1
T124	RHS	0	0	1
T76	RHS	1	1	1
T75	RHS	0	0	1
T72	RHS	0	0	0
T71	RHS	0	0	0
T70	RHS	0	0	1
T63	RHS	0	0	1
T61	RHS	0	0	0
Broion	BR	1	1	1

SOM Table S18.

Raw data for analysis using code in SOM S8.

	taxon	MD	BL
Engis	NEA	5.76	5.78
ROC_DE_MARSAL	NEA	6.28	6.38
KrapinaD23	NEA	6.50	6.61
La_Quina	NEA	5.69	6.14
Kebara_KMH22	NEA	5.99	6.45
Qafzeh15	EHS	6.40	5.73
Qafzeh12	EHS	5.80	6.06
Pavlov13	UPHS	5.46	5.45
Pavlov14	UPHS	5.30	5.05
Dente_T64	RHS	5.48	5.63
Dente_T43	RHS	4.79	5.00
Dente_T16	RHS	5.56	5.09
Dente_3b	RHS	5.42	5.02
Dente_3a	RHS	5.39	5.19
Dente_2b	RHS	5.69	5.68
Dente_1b	RHS	5.02	4.94
Dente_1	RHS	4.81	4.96
Dente_T54	RHS	5.10	5.64
Dente_T53	RHS	5.45	5.91
Dente4	RHS	5.91	5.61
DenteT124	RHS	5.31	4.90
Dente_T76	RHS	5.18	5.54
Dente_T75	RHS	6.24	5.60
Dente_T72	RHS	5.07	5.73
Dente_T71	RHS	4.41	5.46
Dente_T70	RHS	4.81	5.06
Dente_T63	RHS	5.26	5.60
Dente_T61	RHS	5.30	5.78
Dente_T48	RHS	5.58	6.21

SOM File
e-Component
SOM_File_S1.R

```
explore<-function(data, colvar1, colvar2){

cn<-colnames(data)
pdf(paste("reference", "boxplot", cn[colvar1], cn[colvar2], ".pdf",sep="_"), width=20, height=7)
boxplot(data[,colvar1]~data[,colvar2],data)
dev.off()

print(kruskal.test(data[,colvar1]~data[,colvar2],data))

mw_test_res<-matrix(NA, length(levels(data[,colvar2])),length(levels(data[,colvar2])))
rownames(mw_test_res)<-levels(data[,colvar2])
colnames(mw_test_res)<-levels(data[,colvar2])

        for(i in 1:length(levels(data[,colvar2]))){
                for(j in 1:length(levels(data[,colvar2]))){

                                mw_test_res[i,j]<-
wilcox.test(data[data[,colvar2]==levels(data[,colvar2])[i],colvar1],data[data[,colvar2]==levels(data[
,colvar2])[j],colvar1],paired=F,exact=F)$p.value


#print(wilcox.test(data[data[,colvar2]==levels(data[,colvar2])[i],colvar1],data[data[,colvar2]==level
s(data[,colvar2])[j],colvar1],paired=F,exact=F)$statistic)
                }
        }
a<-round(as.dist(mw_test_res),4)
b<-p.adjust(as.vector(a),"bonferroni")
c<-list(a,b)
return(c)


}
```

e-Component
SOM_File_S2.R

```
ttest1ob<-function(x,y){#x=single observation; y=reference

meanref<-mean(y) #compute mean of y
sdref<-sd(y) # compute sd of y
nref<-length(y)
dfref<-length(y)-1
```

```
#compute test statistic following the formula by Sokal and Rohlf 1995:228 modified by Madrigal 2012:116
t<-(x-meanref)/(sdref*(sqrt((nref+1)/nref)))

#compute p of obtaining an equal or more extreme (higher) value than the one obtained with empirical data

pt<-ifelse(t>0,pt(t, df=nref-1,lower.tail=F),pt(t, df=nref-1,lower.tail=T))


print("Test Statistic")
print(t)
print("p of obtaining a more extreme value")
print(pt)
print("Df")
print(dfref)
}
```

e-Component
SOM_File_S3.R

```
quantileValues<-function(x,y){# x=table of values of buccal enamel thikness; y=list of BCD values

list_ind<-split(x, x$ID)
mat<-matrix(NA,length(list_ind),5)
colnames(mat)<-c("0","0.25","0.5","mean","0.75")
rownames(mat)<-rownames(summary(list_ind))

for(i in 1:length(list_ind)){
        for(j in 1:5){


micdist<-(nrow(list_ind[[i]])-1) * 100
#print(micdist)
ind<-cbind(list_ind[[i]], dist=seq(0,micdist, 100))
#print(ind)
mat[i,j]<-ind[which.min(abs(seq(0,micdist, 100) - (quantile(0:y[i,2])[j]))),4]
#print(mat)

        }

}


return(mat)
```

}

SOM File captions

SOM File S1. R source code for calculating Kruskal-Wallis test and pairwise Mann-Whitney test with Bonferroni correction.

SOM File S2. R source code for calculating one-tailed t-test for comparison of a single observation with the mean of a sample (following Sokal and Rohlf, 1995 and Madrigal, 2012).

SOM File S3. R source code for calculating and extracting the values corresponding to the first, second (median), and third quartile of the distance between the cervical plane and the 100 µm bin closest to the bicervical diameter.

SOM References

Andrews, R.M., Kubacka, I., Chinnery, P.F., Lightowlers, R.N., Turnbull, D.M., Howell, N., 1999. Reanalysis and revision of the Cambridge reference sequence for human mitochondrial DNA. Nature Genetics 23, 147.

Arnason, U., Xu, X., Gullberg, A., 1996. Comparison between the complete mitochondrial DNA sequences of *Homo* and the common chimpanzee based on nonchimeric sequences. Journal of Molecular Evolution 42, 145-152.

Arsuaga, J.L., Martínez, I., Arnold, L.J., Aranburu, A., Gracia-Téllez, A., Sharp, W.D., Quam, R.M., Falguères, C., Pantoja-Pérez, A., Bischoff, J., Poza-Rey, E., Parés, J.M., Carretero, J.M., Demuro, M., Lorenzo, C., Sala, N., Martinón-Torres, M., García, N., Alcázar de Velasco, A., Cuenca-Bescós, G., Gómez-Olivencia, A., Moreno, D., Pablos, A., Shen, C.C., Rodríguez, L., Ortega, A.I., García, R., Bonmatí, A., Bermúdez de Castro, J.M., Carbonell, E., 2014. Neandertal roots: Cranial and chronological evidence from Sima de los Huesos. Science 344, 1358-1363.

Becam G, Chevalier T., 2019. Neandertal features of the deciduous and permanent teeth from Portel-Ouest Cave (Ariège, France). American Journal of Physical Anthropology 168, 45–69.

Bentley, D.R., Balasubramanian, S., Swerdlow, H.P., Smith, G.P., Milton, J., Brown, C.G., Hall, K.P., Evers, D.J., Barnes, C.L., Bignell, H.R., Boutell, J.M., Bryant, J., Carter, R.J., Keira Cheetham, R., Cox, A.J., Ellis, D.J., Flatbush, M.R., Gormley, N.A., Humphray, S.J., Irving, L.J., Karbelashvili, M.S., Kirk, S.M., Li, H., Liu, X., Maisinger, K.S., Murray, L.J., Obradovic, B., Ost, T., Parkinson, M.L., Pratt, M.R., Rasolonjatovo, I.M., Reed, M.T., Rigatti, R. Rodighiero, C., Ross, M.T., Sabot, A., Sankar, S.V., Scally, A., Schroth, G.P., Smith, M.E., Smith, V.P., Spiridou, A., Torrance, P.E., Tzonev, S.S., Vermaas, E.H., Walter, K., Wu, X., Zhang, L., Alam, M.D., Anastasi, C., Aniebo, I.C., Bailey, D.M., Bancarz, I.R., Banerjee, S., Barbour, S.G., Baybayan, P.A., Benoit, V.A., Benson, K.F., Bevis, C., Black, P.J., Boodhun, A., Brennan, J.S., Bridgham, J.A., Brown, R.C., Brown, A.A., Buermann, D.H., Bundu, A.A., Burrows, J.C., Carter, N.P., Castillo, N., Chiara, E., Catenazzi, M., Chang, S., Neil Cooley, R., Crake, N.R., Dada, O.O., Diakoumakos, K.D., Dominguez-Fernandez, B., Earnshaw, D.J., Egbujor, U.C., Elmore, D.W., Etchin, S.S., Ewan, M.R., Fedurco, M., Fraser, L.J., Fuentes Fajardo, K.V., Scott Furey, W., George, D., Gietzen, K.J., Goddard, C.P., Golda, G.S., Granieri, P.A., Green, D.E., Gustafson, D.L., Hansen, N.F., Harnish, K., Haudenschild, C.D., Heyer, N.I., Hims, M.M., Ho, J.T., Horgan, A.M., Hoschler, K., Hurwitz, S., Ivanov, D.V., Johnson, M.Q., James, T., Huw Jones, T.A., Kang, G.D., Kerelska, T.H., Kersey,

A.D., Khrebtukova, I., Kindwall, A.P., Kingsbury, Z., Kokko-Gonzales, P.I., Kumar, A., Laurent, M.A., Lawley, C.T., Lee, S.E., Lee, X., Liao, A.K., Loch, J.A., Lok, M., Luo, S., Mammen, R.M., Martin, J.W., McCauley, P.G., McNitt, P., Mehta, P., Moon, K.W., Mullens, J.W., Newington, T., Ning, Z., Ling Ng, B., Novo, S.M., O'Neill, M.J., Osborne, M.A., Osnowski, A., Ostadan, O., Paraschos, L.L., Pickering, L., Pike, A.C., Pike, A.C., Chris Pinkard, D., Pliskin, D.P., Podhasky, J., Quijano, V.J., Raczy, C., Rae, V.H., Rawlings, S.R., Chiva Rodriguez, A., Roe, P.M., Rogers, J., Rogert Bacigalupo, M.C., Romanov, N., Romieu, A., Roth, R.K., Rourke, N.J., Ruediger, S.T., Rusman, E., Sanches-Kuiper, R.M., Schenker, M.R., Seoane, J.M., Shaw, R.J., Shiver, M.K., Short, S.W., Sizto, N.L., Sluis, J.P., Smith, M.A., Ernest Sohna Sohna, J., Spence, E.J., Stevens, K., Sutton, N., Szajkowski, L., Tregidgo, C.L., Turcatti, G., Vandevondele, S., Verhovsky, Y., Virk, S.M., Wakelin, S., Walcott, G.C., Wang, J., Worsley, G.J., Yan, J., Yau, L., Zuerlein, M., Rogers, J., Mullikin, J.C., Hurles, M.E., McCooke, N.J., West, J.S., Oaks, F.L., Lundberg, P.L., Klenerman, D., Durbin, R., Smith, A.J., 2008. Accurate whole human genome sequencing using reversible terminator chemistry. Nature 456, 53-59.

Bouckaert, R., Heled, J., Kühnert, D., Vaughan, T., Wu, C.-H., Xie, D., Suchard, M.A., Rambaut, A., Drummond, A.J., 2014. BEAST 2: a software platform for Bayesian evolutionary analysis. PLoS Computational Biology 10, e1003537.

Briggs, A.W., Good, J.M., Green, R.E., Krause, J., Maricic, T., Stenzel, U., Lalueza-Fox, C., Rudan, P., Brajkovic, D., Kucan, Z., Gusic, I., Schmitz, R., Doronichev, V.B., Golovanova, L.V., de la Rasilla, M., Fortea, J., Rosas, A., Pääbo, S., 2009. Targeted retrieval and analysis of five Neandertal mtDNA genomes. Science 325, 318-321.

Briggs, A.W., Stenzel, U., Johnson, P.L., Green, R.E., Kelso, J., Prüfer, K., Meyer, M., Krause, J., Ronan, M.T., Lachmann, M., Pääbo, S., 2007. Patterns of damage in genomic DNA sequences from a Neandertal. Proceedings of the National Academy of Sciences USA 104, 14616-14621.

Brown S., Higham, T., Slon, V., Pääbo, S., Meyer, M., Douka, K., Brock, F., Comeskey, D., Procopio, N., Shunkov, M., Derevianko A., Buckley, M., 2016. Identification of a new hominin bone from Denisova Cave, Siberia using collagen fingerprinting and mitochondrial DNA analysis. Scientific Reports 6, 23559.

Dabney, J., Meyer, M., 2012. Length and GC-biases during sequencing library amplification: a comparison of various polymerase-buffer systems with ancient and modern DNA sequencing libraries. Biotechniques 52, 87-94.

Dabney, J., Knapp, M., Glocke, I., Gansauge, M.-T., Weihmann, A., Nickel, B., Valdiosera, C., García, N., Pääbo, S., Arsuaga, J.-L., Meyer, M., 2013. Complete mitochondrial genome sequence of a Middle Pleistocene cave bear reconstructed from ultrashort DNA fragments. Proceedings of the National Academy of Sciences USA 110, 15758-15763.

DeAngelis, M.M., Wang, D.G., Hawkins, T.L., 1995. Solid-phase reversible immobilization for the isolation of PCR products. Nucleic Acids Research 23, 4742-4743.

Ermini, L., Olivieri, C., Rizzi, E., Corti, G., Bonnal, R., Soares, P., Luciani, S., Marota, I., De Bellis, G., Richards, M.B., Rollo, F., 2008. Complete mitochondrial genome sequence of the Tyrolean Iceman. Current Biology 18, 1687-1693.

Fu, Q., Meyer, M., Gao, X., Stenzel, U., Burbano, H.A., Kelso, J., Pääbo, S., 2013a. DNA analysis of an early modern human from Tianyuan Cave, China. Proceedings of the National Academy of Sciences USA 110, 2223-2227.

Fu, Q., Mittnik, A., Johnson, P.L.F., Bos, K., Lari, M., Bollongino, R., Sun, C., Giemsch, L., Schmitz, R., Burger, J., Ronchitelli, A.M., Martini, F., Cremonesi, R.G., Svoboda, J., Bauer, P., Caramelli, D., Castellano, S., Reich, D., Pääbo, S., Krause, J., 2013b. A revised timescale for human evolution based on ancient mitochondrial genomes. Current Biology 23, 553-559.

Fu, Q., Li, H., Moorjani, P., Jay, F., Slepchenko, S.M., Bondarev, A.A., Johnson, P.L., Aximu-Petri, A., Prüfer, K., de Filippo, C., Meyer, M., Zwyns, N., Salazar-García, D.C., Kuzmin, Y.V., Keates, S.G., Kosintsev, P.A., Razhev, D.I., Richards, M.P., Peristov, N.V., Lachmann, M., Douka, K., Higham, T.F., Slatkin, M., Hublin, J.-J., Reich, D., Kelso, J., Viola, T.B., Pääbo, S., 2014. Genome sequence of a 45,000-year-old modern human from western Siberia. Nature 514, 445-449.

Frayer, D.W., 1978. Evolution of the detention in upper Paleolithic and Mesolithic Europe. University of Kansas Edition, Lawrence.

Gansauge, M.T., Meyer, M., 2013. Single-stranded DNA library preparation for the sequencing of ancient or damaged DNA. Nature Protocol 8, 737-748.

Gansauge, M.T., Meyer, M., 2014. Selective enrichment of damaged DNA molecules for ancient genome sequencing. Genome Research 24, 1543-1549.

Gansauge, M.T., Gerber, T., Glocke, I., Korlevic, P., Lippik, L., Nagel, S., Riehl, L.M., Schmidt, A., Meyer, M., 2017. Single-stranded DNA library preparation from highly degraded DNA using T4 DNA ligase. Nucleic Acids Research 45, e79.

Gilbert, M.T., Kivisild, T., Grønnow, B., Andersen, P.K., Metspalu, E., Reidla, M., Tamm, E., Axelsson, E., Götherström, A., Campos, P.F., Rasmussen, M., Metspalu, M., Higham, T.F., Schwenninger, J.L., Nathan, R., De Hoog, C.J., Koch, A., Møller, L.N., Andreasen, C., Meldgaard, M., Villems, R., Bendixen, C., Willerslev, E., 2008. Paleo-Eskimo mtDNA genome reveals matrilineal discontinuity in Greenland. Science 320, 1787-1789.

Glocke, I., Meyer, M., 2017. Extending the spectrum of DNA sequences retrieved from ancient bones and teeth. Genome Research 27, 1230-1237.

Green, R.E., Malaspinas, A.S., Krause, J., Briggs, A.W., Johnson, P.L., Uhler, C., Meyer, M., Good, J.M., Maricic, T., Stenzel, U., Prüfer, K., Siebauer, M., Burbano, H.A., Ronan, M., Rothberg, J.M., Egholm, M., Rudan, P., Brajković, D., Kućan, Z., Gusić, I., Wikström, M., Laakkonen, L., Kelso, J., Slatkin, M., Pääbo, S., 2008. A complete Neandertal mitochondrial genome sequence determined by high-throughput sequencing. Cell 134, 416-426.

Hajdinjak, M., Fu, Q., Hübner, A., Petr, M., Mafessoni, F., Grote, S., Skoglund, P., Narasimham, V., Rougier, H., Crevecoeur, I., Semal, P., Soressi, M., Talamo, S., Hublin, J.-J., Gušić, I., Kućan, Ž., Rudan, P., Golovanova, L.V., Doronichev, V.B., Posth, C., Krause, J., Korlević, P., Nagel, S., Nickel, B., Slatkin, M., Patterson, N., Reich, D., Prüfer, K., Meyer, M., Pääbo S., Kelso, J., 2018. Reconstructing the genetic history of late Neanderthals. Nature 555, 652-656.

Ingman, M., Kaessmann, H., Pääbo, S., Gyllensten, U., 2000. Mitochondrial genome variation and the origin of modern humans. Nature 408, 708-713.

Korlević, P., Gerber, T., Gansauge, M.T., Hajdinjak, M., Nagel, S., Aximu-Petri, A., Meyer, M., 2015. Reducing microbial and human contamination in DNA extractions from ancient bones and teeth. Biotechniques 59, 87-93.

Krause, J., Briggs, A.W., Kircher, M., Maricic, T., Zwyns, N., Derevianko, A., Pääbo, S., 2010. A complete mtDNA genome of an early modern human from Kostenki, Russia. Current Biology 20, 231-236.

Krause, J., Krause, J., Fu, Q., Good, J.M., Viola, B., Shunkov, M.V., Derevianko, A.P., Pääbo, S., 2010. The complete mitochondrial DNA genome of an unknown hominin from southern Siberia. Nature 464, 894-897.

Li, H., Durbin, R., 2010. Fast and accurate long-read alignment with Burrows–Wheeler transform. Bioinformatics 26, 589–595.

Meyer, M., Fu, Q., Aximu-Petri, A., Glocke, I., Nickel, B., Arsuaga,J.-L., Martínez, I., Gracia, A., Bermúdez de Castro, J.M., Carbonell, E., Pääbo, S., 2014. A mitochondrial genome sequence of a hominin from Sima de los Huesos. Nature 505, 403-406.

Meyer, M., Kircher, M., Gansauge, M.T., Li, H., Racimo, F., Mallick, S., Schraiber, J.G., Jay, F., Prüfer, K., de Filippo, C., Sudmant, P.H., Alkan, C., Fu, Q., Do, R., Rohland, N., Tandon, A., Siebauer, M., Green, R.E., Bryc, K., Briggs, A.W., Stenzel, U., Dabney, J., Shendure, J., Kitzman, J., Hammer, M.F., Shunkov, M.V., Derevianko, A.P., Patterson, N., Andrés, A.M., Eichler, E.E., Slatkin, M., Reich, D., Kelso, J., Pääbo, S., 2012. A high-coverage genome sequence from an archaic Denisovan individual. Science 338, 222-226.

Molnar, S., 1971. Human tooth wear, tooth function and cultural variability. American Journal of Physical Anthropology 34, 175-189.

Peyrégne, S., Slon, V., Mafessoni, F., de Filippo, C., Hajdinjak, M., Nagel, S., Nickel, B., Essel, E., Le Cabec, A., Wehrberger, K., Conard, N.J., Kind, C.J., Posth, C., Krause, J., Abrams, G., Bonjean, D., Di Modica, K., Toussaint, M., Kelso., J., Meyer, M., Pääbo, S., Prüfer, K., 2019. Nuclear DNA from two early Neandertals reveals 80,000 years of genetic continuity in Europe. Science Advances 5, eaaw5873.

Posth, C., Wißing, C., Kitagawa, K., Pagani, L., van Holstein, L., Racimo, F., Wehrberger, K., Conard, N.J., Kind, C.J., Bocherens, H., Krause, J., 2017. Deeply divergent archaic mitochondrial genome provides lower time boundary for African gene flow into Neanderthals. Nature Communications 8, 16046.

Prüfer, K., de Filippo, C., Grote, S., Mafessoni, F., Korlević, P., Hajdinjak, M., Vernot, B., Skov, L., Hsieh, P., Peyrégne, S., Reher, D., Hopfe, C., Nagel, S., Maricic, T., Fu, Q., Theunert, C., Rogers, R., Skoglund, P., Chintalapati, M., Dannemann, M., Nelson, B.J., Key, F.M., Rudan, P., Kućan, Ž., Gušić, I., Golovanova, L.V., Doronichev, V.B., Patterson, N., Reich, D., Eichler, E.E., Slatkin, M., Schierup, M.H., Andrés, A.M., Kelso, J., Meyer, M., Pääbo, S., 2017. A high-coverage Neandertal genome from Vindija Cave in Croatia. Science 358, 655-658.

Prüfer, K., Racimo, F., Patterson, N., Jay, F., Sankararaman, S., Sawyer, S., Heinze, A., Renaud, G., Sudmant, P.H., de Filippo, C., Li, H., Mallick, S., Dannemann, M., Fu, Q., Kircher, M., Kuhlwilm, M., Lachmann, M., Meyer, M., Ongyerth, M., Siebauer, M., Theunert, C., Tandon, A., Moorjani, P., Pickrell, J., Mullikin, J.C., Vohr, S.H., Green, R.E., Hellmann, I., Johnson, P.L.F., Blanche, H., Cann, H., Kitzman, J.O., Shendure, J., Eichler, E.E., Lein, E.S., Bakken, T.E., Golovanova, L.V.,

Doronichev, V.B., Shunkov, M.V., Derevianko, A.P., Viola, B., Slatkin, M., Reich, D., Kelso, J., Pääbo, S., 2014. The complete genome sequence of a Neanderthal from the Altai Mountains. Nature 505, 43-49.

Reich, D., Green, R.E., Kircher, M., Krause, J., Patterson, N., Durand, E.Y., Viola, B. Briggs, A.W., Stenzel, U., Johnson, P.L., Maricic, T., Good, J.M., Marques-Bonet, T., Alkan, C., Fu, Q., Mallick, S., Li, H., Meyer, M., Eichler, E.E., Stoneking, M., Richards, M., Talamo, S., Shunkov, M.V., Derevianko, A.P., Hublin, J.J., Kelso, J., Slatkin, M., Paabo, S., 2010. Genetic history of an archaic hominin group from Denisova Cave in Siberia. Nature 468, 1053-1060.

Renaud, G., Stenzel, U., Kelso, J., 2014. leeHom: adaptor trimming and merging for Illumina sequencing reads. Nucleic Acids Research 42, e141.

Rohland, N., Glocke, I., Aximu-Petri, A., Meyer, M., 2018. Extraction of highly degraded DNA from ancient bones, teeth and sediments for high-throughput sequencing. Nature Protocols 13, 2447-2461.

Rougier, H., Crevecoeur, I., Beauval, C., Posth, C., Flas, D., Wißing, C., Furtwängler, A., Germonpré, M., Gómez-Olivencia, A., Semal, P., van der Plicht, J., Bocherens, H., Krause, J., 2016. Neandertal cannibalism and Neandertal bones used as tools in Northern Europe. Scientific Reports 6, 29005.

Santorum, J.M., Darriba, D., Taboada, G. L., Posada, D., 2014. jmodeltest.org: selection of nucleotide substitution models on the cloud. Bioinformatics 30, 1310-1311.

Sawyer, S., Renaud, G., Viola, B., Hublin, J.-J., Gansauge, M.-T., Shunkov, M.V., Derevianko, A.P., Prüfer, K., Kelso, J., Pääbo, S., 2015. Nuclear and mitochondrial DNA sequences from two Denisovan individuals. Proceedings of the National Academy of Sciences USA 112, 15696-15700.

Skoglund, P., Northoff, B.H., Shunkov, M.V., Derevianko, A.P., Pääbo, S., Krause, J., Jakobsson, M., 2014. Separating endogenous ancient DNA from modern day contamination in a Siberian Neandertal. Proceedings of the National Academy of Sciences USA 111, 2229-2234.

Slon, V., Viola, B., Renaud, G., Gansauge, M.-T., Benazzi, S., Sawyer, S., Hublin, J.-J., Shunkov, M.V., Derevianko, A.P., Kelso, J., Prüfer, K., Meyer, M., Pääbo, S., 2017a. A fourth Denisovan individual. Science Advances 3, e1700186.

Slon, V., Hopfe, C., Weiß, C.L., Mafessoni, F., de la Rasilla, M., Lalueza-Fox, C., Rosas, A., Soressi, M., Knul, M.V, Miller, R., Stewart, J.R., Derevianko, A.P., Jacobs, Z., Li, B., Roberts, R.G., Shunkov, M.V., de Lumley, H., Perrenoud, C., Gušić, I., Kućan, Ž., Rudan, P., Aximu-Petri, A.,

Essel, E., Nagel, S., Nickel, B., Schmidt, A., Prüfer, K., Kelso, J., Burbano, H.A., Pääbo, S., Meyer, M., 2017b. Neandertal and Denisovan DNA from Pleistocene sediments. Science 356, 605-608.

Smith, B.H., 1984. Patterns of molar wear in hunter-gatherers and agriculturists. American Journal Physical Anthropology 63, 39-56.

Tamura, K., Nei, M., 1993. Estimation of the number of nucleotide substitutions in the control region of mitochondrial DNA in humans and chimpanzees. Molecular Biology and Evolution 10, 512-526.

Turner, C.G., Nichol, C.R., Scott, G.R., 1991. Scoring procedures for key morphological traits of the permanent dentition: the Arizona State University dental anthropology system. In: Kelley, M.A., Larsen, C.S. (Eds.), Advances in Dental Anthropology. Wiley-Liss, New York, pp. 13-31.

Voisin, J. L., Condemi, S., Wolpoff, M. H., Frayer, D. W., 2012. A new online database (http://anthropologicaldata.free.fr) and a short reflection about the productive use of compiling internet data. PaleoAnthropology 2012, 241–244.

Wood, R.E., Higham, T.F.G., De Torres, T., Tisnérat-Laborde, N., Valladas, H., Ortiz, J.E., Lalueza-Fox, C., Sánchez-Moral, S., Cañaveras, J.C., Rosas, A., Santamaría, D., De La Rasilla, M., 2013. A new date for the Neanderthals from El Sidrón Cave (Asturias, northern Spain). Archaeometry 55, 148-158.